SELF-INDUCED CHATTER VIBRATION OF LATHE TOOLS

by

MUNG CHEN

B.S., California State University at Sacramento, 1972

A THESIS SUBMITTED IN PARTIAL FULFILMENT OF

THE REQUIREMENTS FOR THE DEGREE OF

MASTER OF APPLIED SCIENCE

in the Department

of

Mechanical Engineering

We accept this thesis as conforming

to the required standard

THE UNIVERSITY OF BRITISH COLUMBIA

August, 1974

In presenting this thesis in partial fulfilment of the requirements for an advanced degree at the University of British Columbia, I agree that the Library shall make it freely available for reference and study. I further agree that permission for extensive copying of this thesis for scholarly purposes may be granted by the Head of my Department or by his representatives. It is understood that copying or publication of this thesis for financial gain shall not be allowed without my written permission.

Department of Mechanical Engineering

The University of British Columbia
Vancouver 8, Canada

Date August 16, 1974

ABSTRACT

Self-excited chatter is a basic performance limitation in the machining of metals. Self-excited chatter was investigated both experimentally and theoretically in the present research. An experimental lathe was constructed so as to obtain orthogonal one degree of freedom cutting. An experimental method developed by Brockley and Ko which enables the recording of a phase plane diagram and the force-velocity curve of one cycle of vibration was used. Experiments were carried out on 70-30 lead free brass workpiece disc with a high speed steel tool at surface speeds ranging from 2 in/sec to 20 in/sec. The results revealed that the force-velocity curve was 'loop' shaped. The chatter vibration was quasi-harmonic and the growth and decay of vibration amplitude with variation in surface speed was observed. Frictional quasi-harmonic vibration was observed to occur in the same speed range which suggested the concept that metal-cutting chatter could be friction actuated. The experimental force-velocity curve was employed in a graphical construction of the phase plane representation of the vibration. The constructed phase plane was in close agreement with the experimental recording.

TABLE OF CONTENTS

Acknowledgement

The author wishes to express thanks to Mr. John Wiebe, for his assistance in constructing the apparatus, Mr. E. Jones, who designed the instrumentation, to the staff of the Mechanical Engineering Laboratory, to the faculty and graduate students in the Department of Mechanical Engineering for their many helpful suggestions.

Special thanks are due to his research supervisor, Dr. C.A. Brockley, for his quidance and constant encouragement.

The experimental work of this thesis was carried out in the Tribology Laboratory. The use of facilities is gratefully acknowledged. Financial Assistance was received from the National Research Council under grant number 67-1065.

LIST OF FIGURES

LIST OF FIGURES (cont.)

NOMENCLATURE

Symbol		Units
e	Cutting force due to initial deflection	lb
f	Frequency of chatter vibration	Hz
m	Equivalent mass of the vibrating parts	lbm
k	Stiftness of Contilever beam	lb/in
r	Damping coefficient	lb sec/in
t	Time	sec
t_1	Depth of cut	in
t_2	Chip thickness	in
x	Displacement of tool bit	in
$\dot{x}$	Velocity of tool bit	in/sec
$\ddot{x}$	Acceleration of tool bit	in/sec^2
A	Amplitude of chatter vibration	in
F	Cutting force	lb
F( )	Force as a function of the bracketed term	lb
$\overline{F}$	Nominal cutting force	lb
v	Surface speed	in/sec
α	Amplitude of friction-induced vibration	in
ω	Damped natural frequency	rad/sec
ω_n	natural frequency	rad/sec
θ	Angular displacement of tool bit	rad

CHAPTER 1

1.1 Introduction

The cutting of metal is frequently accompanied by vibration, commonly known as "chatter". Chatter has adverse effects on the surface finish, dimensional accuracy, tool life, machine life and the rate of production.

Chatter vibrations are generally of two kinds, i.e. forced vibration and self-induced vibration. Den Hartog [1] gives the following definition which serves to distinguish between the two forms of vibration :
"In a self-induced vibration the alternating force that sustains the motion is created or controlled by the motion itself; when the motion stops the alternating force disappears."
"In a forced vibration, the sustaining alternating force exists independently of the motion and persists even when the vibration motion is stopped."

The theory of forced vibration is well developed compared to the self-induced oscillations which arise in non-linear systems. In practice, the source that causes forced vibration can usually be identified by comparing its frequency to that of the chatter frequency. Forced chatter may result from unbalance of rotating members, uneven gear teeth, rough spindle bearings or impacts from a multi-tooth cutter. The surface irregularity or the frequency of vibration will change proportionally to the speed of the machine component which acts as the driving force. The solution to the problem of

forced chatter, once the source is identified, becomes relatively simple.

For the self-induced chatter, it is found that the frequency remains constant, as cutting speed is changed [2]. The frequency is of the same order of magnitude as one of the natural frequencies of one machine component or the workpiece. The violent chatter often observed during cutting has been identified to be of the self-induced type in most cases. Self-induced vibration has been considered as a free vibration with negative damping. An ordinary positive viscous damping force is a force proportional to the velocity of vibration and directly opposed to it. A negative damping force is also proportional to the velocity but has the same direction as the velocity. Instead of diminishing the amplitude of the free vibration, the negative damping gives an increase in amplitude [1]. However, indefinite amplitude growth has never been observed in practice and reached a limit cycle [3, 24, 25]. It must follow from this theory that the damping term varies with cutting conditions during chatter, thus making experimental varification of the theory difficult.

1.2 Historical Background

A literature survey has revealed that little research devoted specifically to the problem of tool vibration was published prior to Arnold [3]. Taylor [4] suggested that the vibration was due to the variable force created by the periodic shearing action occuring as the metal was removed. Dempster [5] measured the periodic force at extremely low cutting speeds and found that the variation decreases and becomes almost negligible

at cutting speeds in excess of 15 ft/min. Doi was one of the earliest workers to consider the cutting process as capable of establishing a self-excited system [6]. He ascribes the vibration to the resonance due to fluctuations of the cutting action synchronizing with a natural frequency of the lathe.

A comprehensive work entitled "Manual on Cutting of Metals" published by the American Society of Mechanical Engineers [7] devoted two pages to "chatter", of which it states "its severity undoubtedly is determined by the degree of resonance between periodic variations in the cutting force and the natural frequencies of the work, and of the work and tool-supporting structures". The general impression gained from the above publications is that tool vibration is due to a recurrent variation of cutting force due to shearing of the chip. No satisfactory explanation is offered for the existence of resonant vibration.

Arnold [3] presented the first systematic study of metal cutting chatter. In the case of self-excited chatter, he observed that the amplitude of vibration appeared to be independent of depth of cut and seemed to be limited to a value slightly in excess of that which makes the maximum vibrational velocity at the tool point equal to the speed of work. He pointed out the self-inducing influence originated from the decrease in the cutting force which occurs as the speed is increased, and becomes more powerful as the wear of the tool progressed. However, Hahn [2] observed that the slope of the force cutting speed curve appeared to be zero in certain speed ranges where chatter vibration is important and disputed

Arnold's argument of negative slope. Other authors have also approached the problem of self-induced vibration by various analog and mathematical models [8, 9, 10, 11, 12].

A major effort to study chatter was carried out and its results published in 1965 under a U.S. Airforce contract, entitled, 'Effects and Control of Chatter Vibration in Machine Tool Processes [13, 14, 15, 16]. A theory was developed which permitted calculation of borderlines of stability for a structure having n-degrees of freedom and assuming no dynamics in the cutting process [13]. He noted, however, that an infinite number of solutions exist for a given machine because the structure dynamics vary with cutting-force orientation. It is therefore, apparent that further fundamental research to investigate the nature of self-induced chatter remains to be done.

The main defect in the force-cutting speed curve which many theories are based upon relates to the use of conventional displacement dynamometer for the measurement of force. However, under vibratory conditions, inertia and damping forces cannot be ignored. Thus, in the present work it was considered that the proper approach was to measure the force dynamically taking into account these effects.

A recent paper by Brockley & Ko [17] "The Measurement of Friction and Friction-Induced Vibration," deals with analogous phenomena. The present work extends the knowledge to the theory of tool chatter.

CHAPTER II

2.1 Theoretical Model

A typical cutting tool and workpiece configuration is shown in Fig. 2.1.1 (refer to section 3.2 for detail). It can be described by a mass-spring-damper model as shown in Fig. 2.1.2 . The configuration of the model is of a typical system which may exhibit self-induced chatter. The elastically constrained cutting tool of equivalent mass m was used to make one-dimensional orthorgonal cutting along the circumference of the disc workpiece which is assumed infinitely stiff and is driven at constant speed 'V'. Elasticity is supplied by the cantilever beam.

Self-induced oscillations are steady state oscillations sustained by forces created by the motion itself and disappear when the motion stops. In the case of metal cutting on a lathe, the force created is the tangential cutting force, which is generally agreed to be dependent on three major variables during vibration: depth of cut, rake angle of cutting tool and cutting speed. If the amplitude of the vibration is small compared to the length of the cantilever beam, it can be shown that the variations in depth of cut and rake angle during vibration may be neglected [3]. The model is then reduced to one where the cutting force depends only on the cutting speed. Cutting speed, properly defined, is the relative velocity between the tool and the workpiece under conditions of chatter vibration. It is not the surface speed of the workpiece as many other workers have presumed.

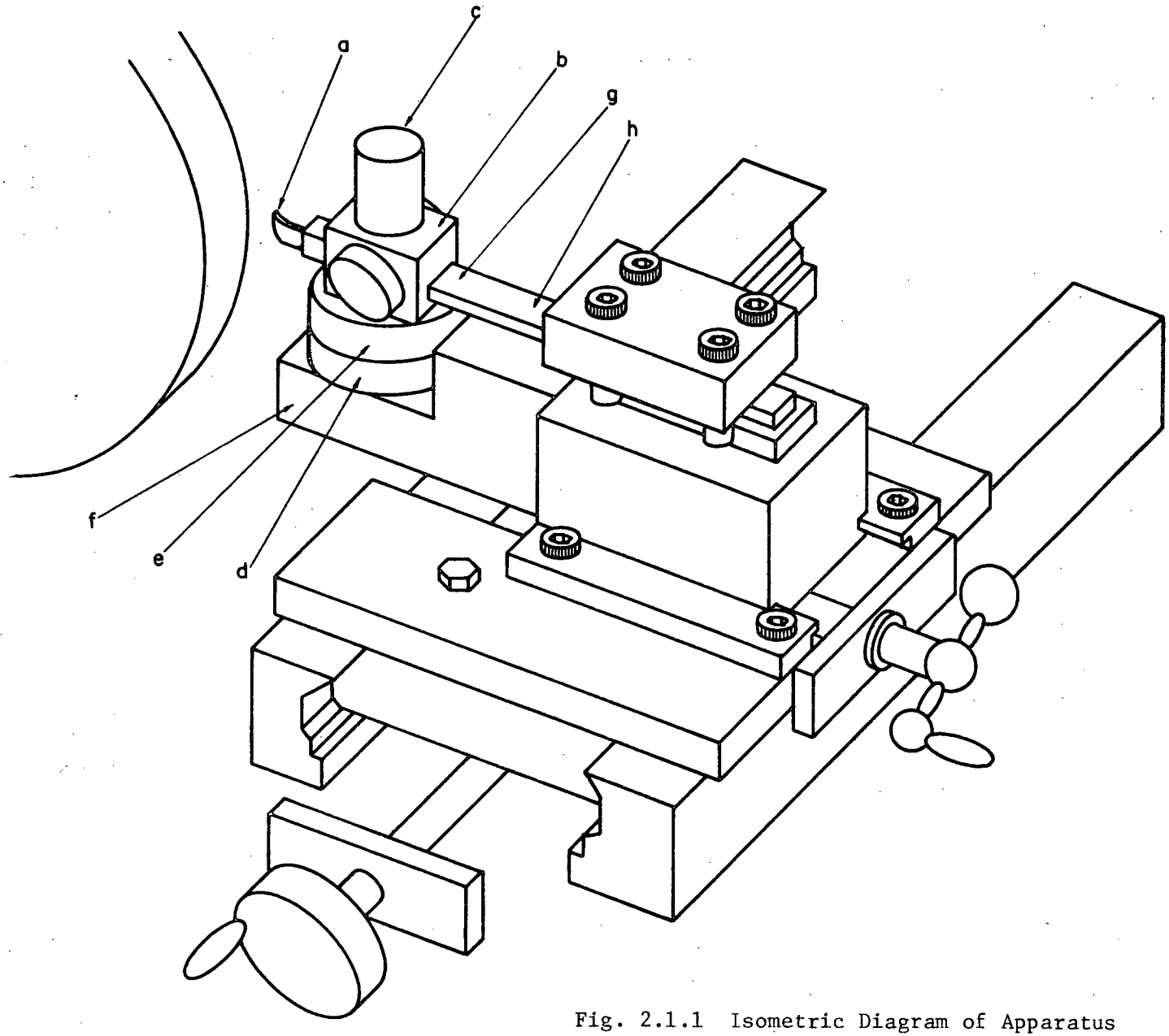

Fig. 2.1.1 Isometric Diagram of Apparatus

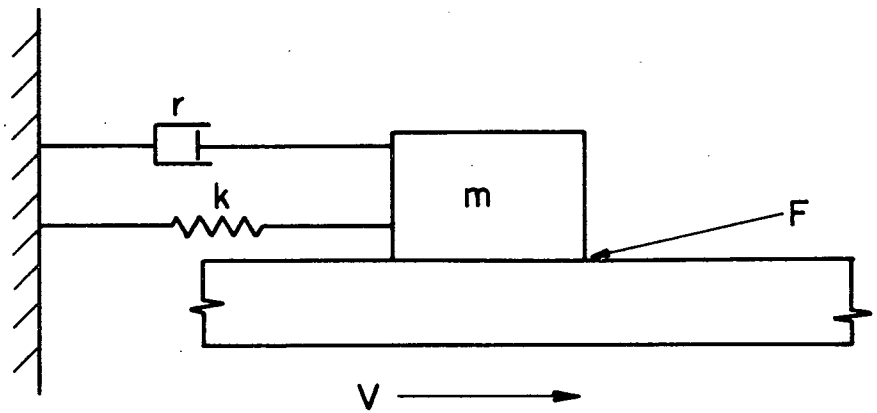

Fig. 2.1.2 Schematic Diagram of Mass-Spring-Damper System

2.2 Energy Consumed in Metal Cutting

Energy consumed in metal cutting can be categorized into : a. Surface energy; b. Shear deformation work in shear zone; c. Frictional energy on the tool face; d. Frictional energy on the tool flank; e. Kinetic energy of the chip [18].

Under usual cutting conditions, the surface energy for new surface formation and the kinetic energy associated with a chip are negligibly small compared with other energies. The shear strength is not known to vary with slip velocity. This suggests that the variation in friction during vibration may be associated with metal cutting chatter.

2.3 The Slope of the Force-Velocity Curve

Consider the cutting force as a function of slip velocity, then

$$m\ddot{x} + r\dot{x} + kx = F(V - \dot{x}) \qquad (1)$$

where $F(V - \dot{x})$ is the cutting force. When this function is expressed in terms of an equation, all the terms involving $\dot{x}$, $\dot{x}^2$, $\dot{x}^3$ etc, can be transferred to the left hand side of the equation, leaving the right hand side with the constant terms in V, the surface speed. If the constant terms is represented by e, then equation (1) can be written as

$$\ddot{x} + \frac{r}{m}\dot{x} - \frac{1}{m}F(\dot{x}) + \frac{k}{m}x = \frac{1}{m}e \qquad (2)$$

where $F(\dot{x})$ is a function of $\dot{x}$.

Letting $y = x - \frac{e}{k}$ and $\omega^2 = \frac{k}{m}$; then

$$\dot{y} = \dot{x} \ , \quad \ddot{y} = \ddot{x}$$

and

$$\frac{k}{m} y = \frac{k}{m} x - \frac{e}{m} \ .$$

Substituting these in equation (2) yields

$$\ddot{y} + \frac{r}{m} \dot{y} - \frac{1}{m} F(\dot{y}) + \omega^2 y = 0 \tag{3}$$

The elimination of the constant term $\frac{e}{m}$ simply means that the tool bit will vibrate around a new position instead of the original static position with the amplitude of vibration remaining the same. The constant term $\frac{e}{k}$ is the initial deflection of the tool bit when cutting starts.

Equation (1) can be considered in an alternative way. Taking $|\dot{x}| << V$ initially, by Taylor's theorem, referred to by McLachlan [22], we get

$$F(V - \dot{x}) \cong F(V) - \dot{x}F'(V) + \frac{1}{2} \dot{x}^2 F''(V) - \frac{1}{6} \dot{x}^3 F'''(V) \tag{4}$$

differentiation being with respect to V. After substituting in equation (1) and dropping the constant term, we get

$$y + \{\frac{r}{m} + \frac{1}{m}[F'(V) - \frac{1}{2} F''(V)\dot{y} + \frac{1}{6} F'''(V)\dot{y}^2]\}\dot{y} + \omega^2 y = 0 \tag{5}$$

Initially when $\dot{y}$ is small, and if r, the system damping, is also relatively small, then the coefficient of $\dot{y}$ is negative since

$F'(V) < 0$, for the case of negative slope of the cutting force-velocity [3] curve, so that the oscillation tends to grow. When the amplitude attains its ultimate value, the coefficient of $\dot{y}$ is alternatively positive and negative, such that the energy supplied from the driven surface is equal to that dissipated. The Taylor's expansion demonstrates the importance of the negative slope of the force-velocity curve.

2.4 Graphical Solution

A method of graphical solution was developed by Dudley and Swift for investigating the effects of varying damping coefficient and changing the driven surface velocity on frictional oscillations [19]. The graphical method makes use of the friction-velocity curve directly thus eliminating the complication of finding a analytical function for the curve. This method is applicable in the case of self-excited chatter once the force velocity curve is obtained. Let

$$\ddot{x} = \frac{d\dot{x}}{dt} = \dot{x} \frac{d\dot{x}}{dx}$$

and substitute into equation (1), we have

$$\dot{x} \frac{d\dot{x}}{dx} + \frac{r}{m} \dot{x} + \frac{k}{m} x = \frac{F}{m} \qquad (6)$$

Rearranging and divide by $\sqrt{k/m}$, equation (6) becomes

$$\sqrt{\frac{k}{m}}\, x - \frac{F - r\dot{x}}{\sqrt{k/m}} = -\dot{x} \frac{d\dot{x}}{dx\sqrt{k/m}}$$

Dividing the cutting force F by $\sqrt{km}$ gives units of velocity. A curve relating the cutting force and the slip velocity can then be plotted as shown in Fig. 2.4.1. Next, a new axis $\sqrt{\frac{k}{m}}\,x$ of the same dimension and scale is established with $0'$ as origin and at a distance V away from the $F/\sqrt{km}$ axis. Finally ABC, the relationship between $\frac{F - r\dot{x}}{\sqrt{km}}$ and the oscillating velocity $\dot{x}$ is obtained by subtracting the system damping effect $r\dot{x}$ throughout the original cutting force vs. velocity curve with $0'$ as origin.

If P represents any momentary condition, so that $RO' = \dot{x}$ and $PR = \sqrt{\frac{k}{m}}\,x$, then it can easily be shown from Fig. 2.4.1 that since

$$PQ = PR - QR$$

and since

$$QR = \frac{F - r\dot{x}}{\sqrt{km}} ,$$

therefore

$$PQ = \sqrt{\frac{k}{m}}\,x - \frac{F - r\dot{x}}{\sqrt{km}} = - \dot{x}\,\frac{d\dot{x}}{dx\sqrt{k/m}} ,$$

also

$$QS = RO' = \dot{x} .$$

Thus

$$\frac{PQ}{RS} = \frac{- \dot{x}\,\frac{d\dot{x}}{dx\sqrt{k/m}}}{\dot{x}} = - \frac{d\dot{x}}{dx\sqrt{k/m}}$$

Hence SP is the radius vector of the trajectory relating $\dot{x}$

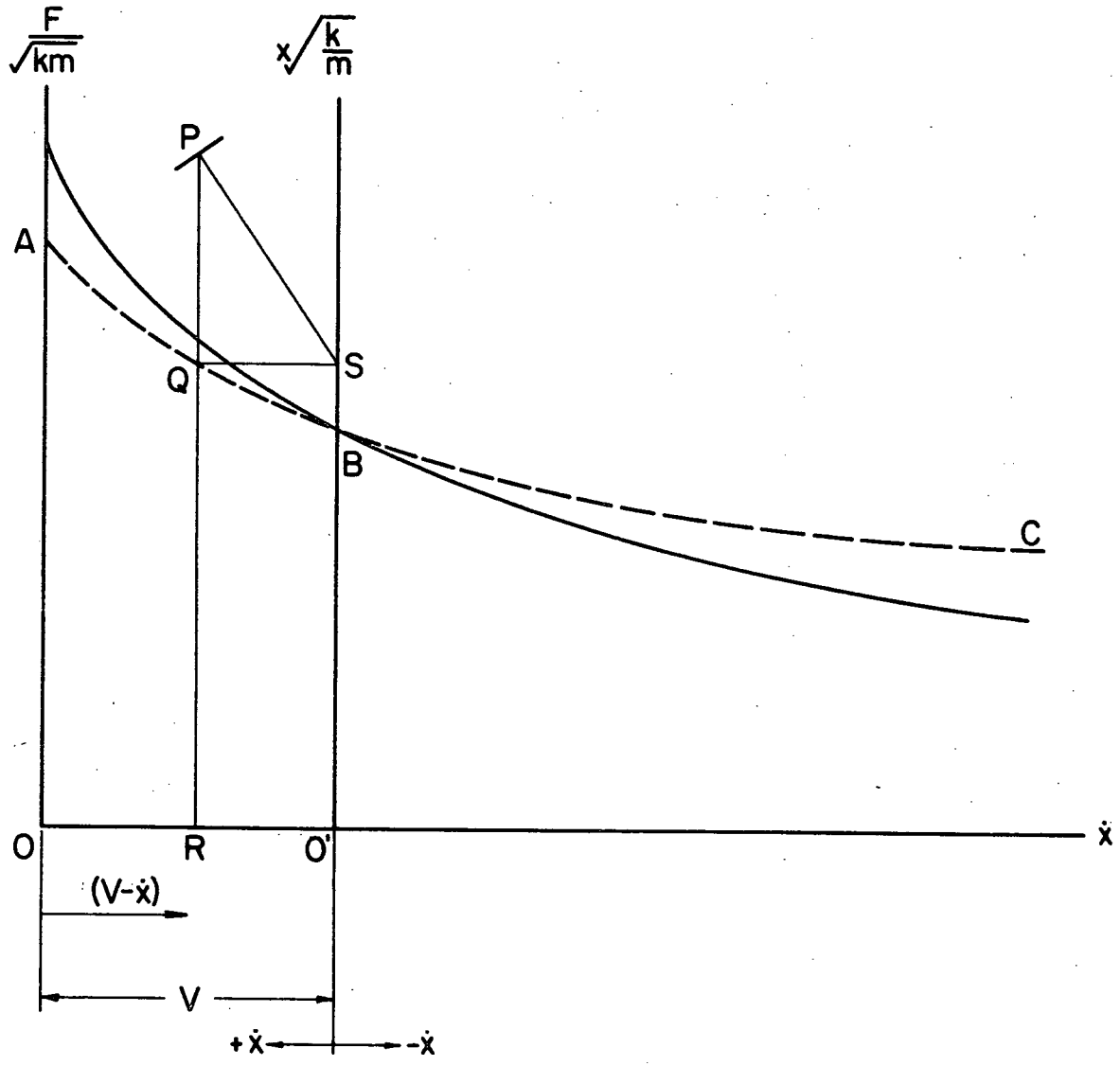

Fig. 2.4.1 Graphical Construction of Phase-Plane Diagram

and $\sqrt{\frac{k}{m}}\,x$ at the point P where its tangent is normal to PS, thus a complete trajectory can be developed by drawing successive tangential elements. The trajectory thus obtained will either spiral inwards or outwards, ultimately being asymtotic to a closed curve. Otherwise the trajectory will spiral continually outward and ultimately reach the $F/\sqrt{km}$ axis. Fig. 2.4.2 shows a graphical construction of a phase trajectory in which the circle ZZ is for stable quasi-sinusoidal oscillations.

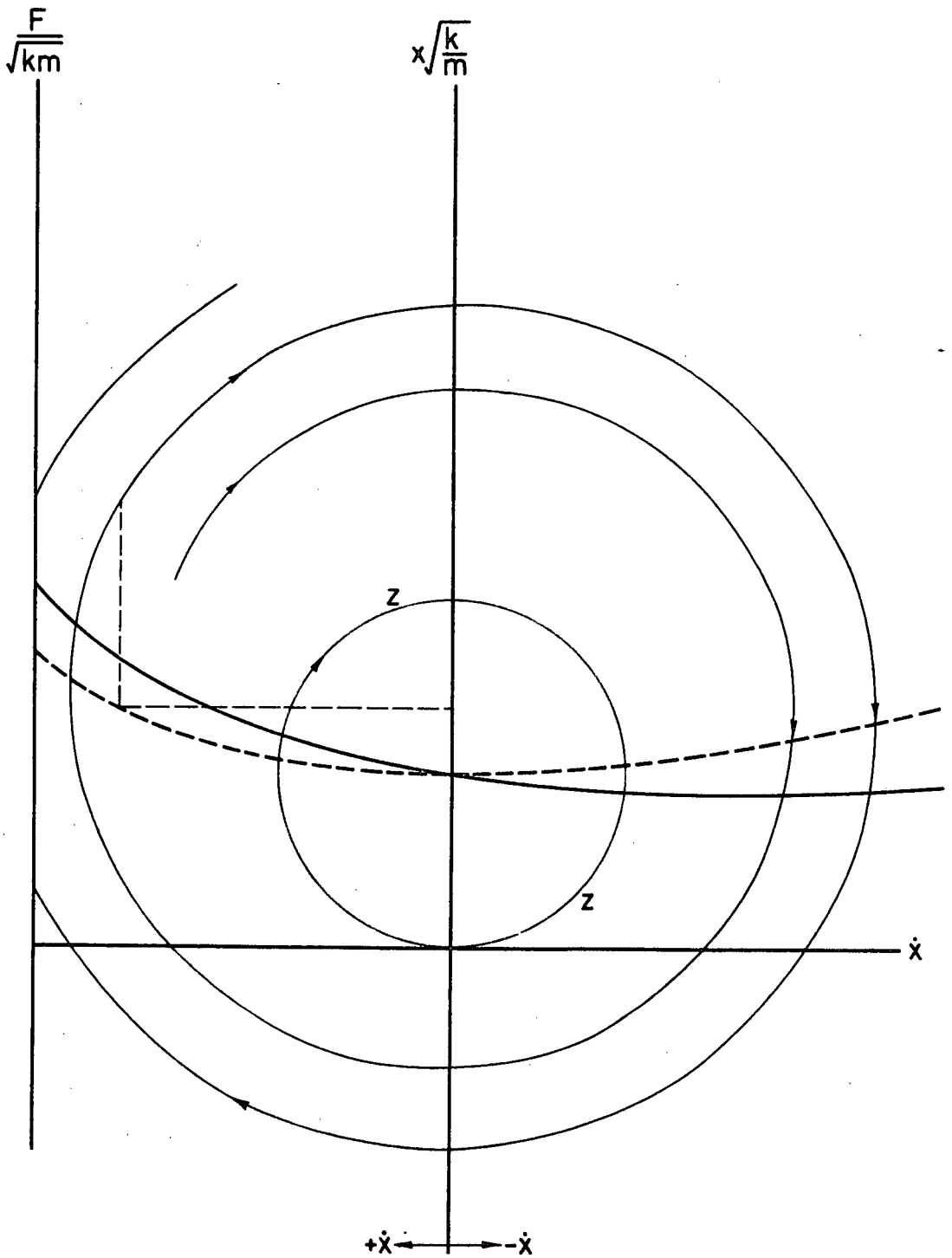

Fig. 2.4.2 Phase Plane Diagram

CHAPTER III

3.1 Experimental Objective

The assessment of cutting force with a conventional dynamometer is done by recording the displacement of the tool bit alone, i.e. by assuming a linear variation of cutting force versus displacement. However, under vibratory conditions this method does not give a true representation of the cutting since inertia force and viscous damping forces must also be considered. The cutting force versus slip velocity curves obtained with this method by previous workers and used as a basis of chatter theories were, in the true sense, a measure of average cutting force versus the surface speed of the workpiece. The use of these results as if they were dynamic force-velocity curves was therefore grossly in error.

The primary objective of the present experiments was to obtain the force velocity curves under dynamic conditions.

3.2 Apparatus

The apparatus used is as shown in Fig. 2.1.1 . The purpose of the design was to construct an experimental lathe which allows only one-degree of freedom for vibration for the cutting tool.

The major variables involved in the investigation were displacement, velocity and acceleration of the tool bit, force and depth of cut and surface speed. Thus, the essential parts of the apparatus consisted of a circular disc as the workpiece, a variable speed drive unit, a

cantilever beam and a feed mechanism. The measurements of the variables will be explained in section 3.3.

As shown in Fig. 2.1.1, the tool bit (a) was clamped to the tool holder (b); the accelerometer (c) fitted on the top and the upper-half of the velocity transducer (e) fitted on the bottom. The lower half (d) was placed on th supporting block (f). The cantilever beam (g) provided the elasticity of the system. Strain gauges (h) were fitted to the top and bottom of the beam at the far end from the tool holder. The beam was clamped onto the supporting block which could be adjusted parallel to the axis of the workpiece by a lead-screw mechanism. (8-threads per inch) Two 3/8-inch diameter bolts were used to secure the block in the desired position. The feed mechanism consisted of a 20-threads per inch lead screw and two guide-rails which could be clamped down by four allen screws when cutting was performed. On Fig. 3.2.1, the driving unit is shown. In order to eliminate the effects of motor vibration on the cutting process, careful isolation techniques were employed. Power was transmitted from the variable speed $1\frac{3}{4}$ H.P. D.C. Motor (i) to the speed reducer (j) by grooved aluminum sheaves (k) and rubber O-rings (ℓ). This type of transmission reduced alignment problems and provided good vibration isolation between the motor and the speed reducer. The speed reducer was a 17:1 worm gear. The bearings of the speed reducer were removed and replaced with brass bushings (m) in order to minimize possible forced vibration due to unbalanced forces in the rolling element. Finally, the cutting apparatus and the speed reducer were placed on a massive concrete block (n) which rested on a solid foundation, which effectively isolated vibration external to the

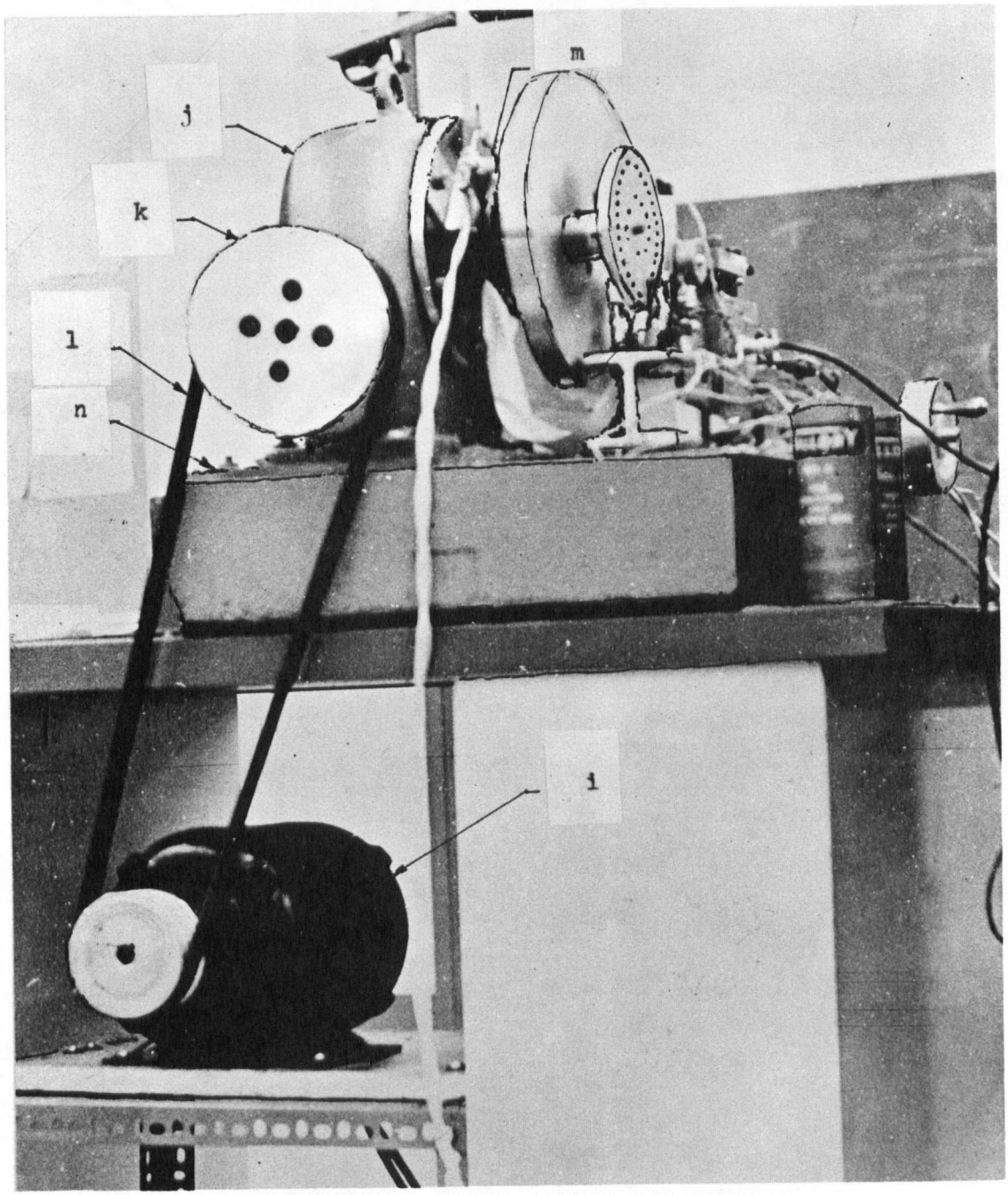

Fig. 3.2.1 Drive Unit

system. The motor had an effective speed range from 50 to 2000 r.p.m. The one-step sheaves used gave a ratio of 1.63:1. When this arrangement was used with the 17:1 speed reducer, a reasonable range of surface speed could be obtained. On a 11 in diameter workpiece, the surface speed had an approximate range of 1 in/sec to 40 in/sec.

3.3 Instrumentation

The investigation required the determination of the cutting force and amplitude of vibration for various values of surface speed and depth of cut.

The conventional method of determining the cutting force characteristics by assuming force as a linear function of displacement does not give accurate information.

Consider the d. e. for a damped free vibration of a mass-spring-damper system as shown in Fig. 2.1.2 :

$$m\ddot{x} + r\dot{x} + kx = 0.$$

This could be written as $r\dot{x} = -(m\ddot{x} + kx)$. If $(m\ddot{x} + kx)$ was plotted against the absolute velocity $\dot{x}$, a straight line was obtained which had slope r.

During self-excited chatter, the following d. e. applies :

$$m\ddot{x} + r\dot{x} + kx = f(V - \dot{x})$$

thus a plot of $(m\ddot{x} + kx)$ against $\dot{x}$ represents the dynamic cutting

force-velocity characteristics which includes the viscous damping force. In practice, scaled accelerometer and displacement signals were fed to the differential amplifier of an oscilloscope, and the velocity signal was introduced to the horizontal differential amplifier. This method gave a realistic assessment of dynamic cutting force.

The general arrangement of the instrument circuitry is shown in Fig. 3.3.1. The details of the various measurements are as follows :

a. Displacement

A 350-ohm strain gauge was cemented to each side of the cantilever beam to measure the displacement of the tool bit. The two strain gauges together with two 350-ohm dummy resistors form a four-arm wheatstone bridge circuit which was connected to a bridge amplifier. The output from the amplifier was channeled to various recording instruments.

b. Velocity

An electromagnetic type transducer was used to record velocity of the vibrating mass. The transducer incorporated a coil having a D. C. resistance of 700 ohms and an inductance of 0.1 henry. The core magnet produced a norminal output on the apparatus of 16.9 mv/(in/sec).

c. Acceleration

A model 305A Kistler servo accelerometer was attached at the top of the tool holder. The accelerometer weighed 3oz and had a dimension of 1 in diameter × 2 in . The accelerometer was a self-contained unit;

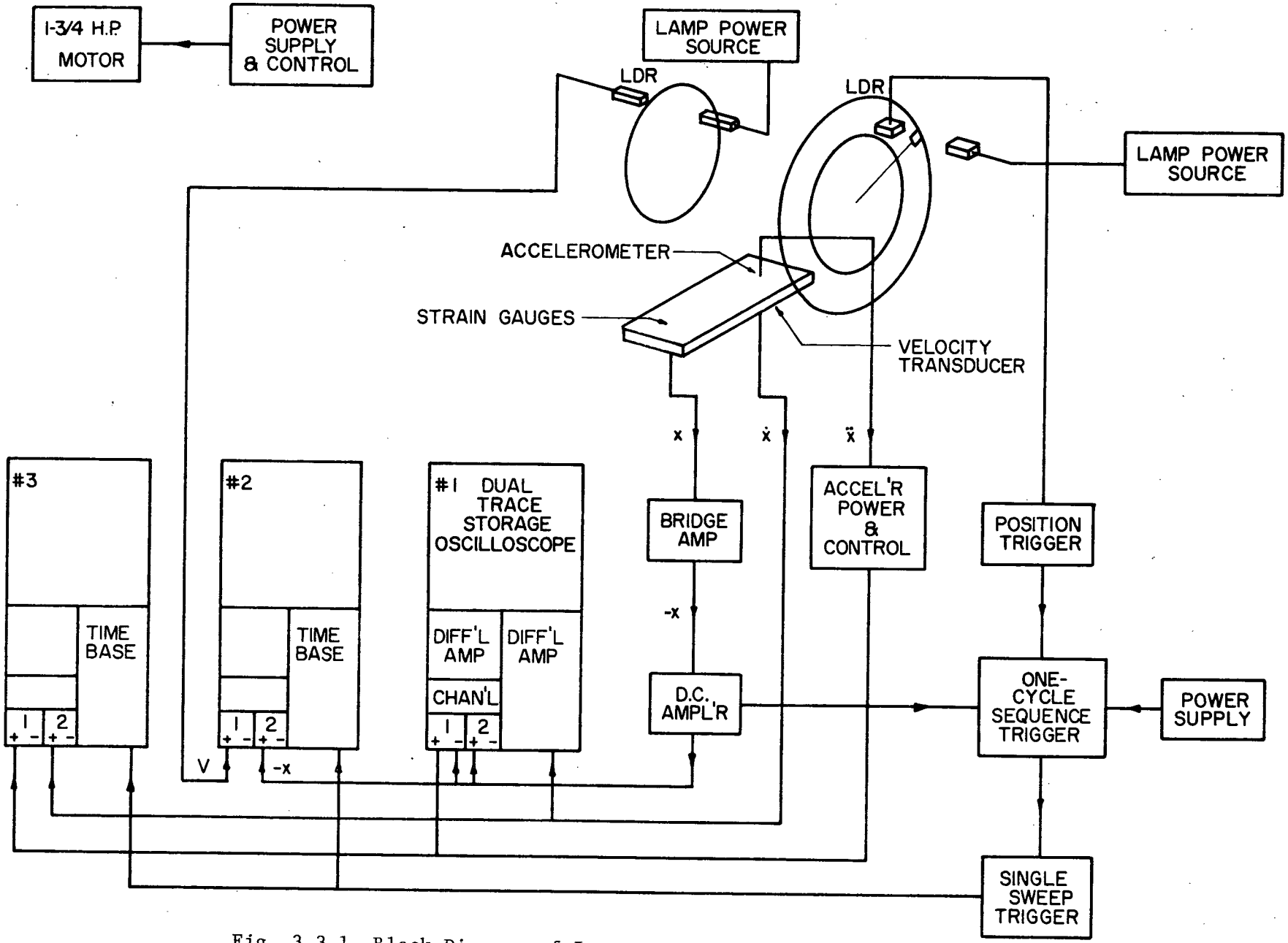

Fig. 3.3.1 Block Diagram of Instrument Circuitry

no amplifier was required and the output was fed directly to the recording instruments. Full scale range was normally set at ± 50g., thus giving a voltage sensitivity of 0.1 volt/g. and a resolution of less than 5 micro. g. The full scale range could be varied by varying an external resistor. The phase shift of the acceleration signal was negligible at 95 Hz , which was the natural frequency of the cantilever beam (Appendix I). The cutting frequency was expected to correspond closely with the natural frequency of the beam.

d. Surface Speed

The speed of the rotating disc was measured by a counting disc and LDR (Light Detecting Resistor) system. The counting system required no driving mechanism thus the counter unit could be placed in a area remote from the cutting apparatus. This procedure minimized the possibility of mechanical noise being picked up by the recording instruments. The counting disc had two rows of 1/8 in. dia. holes. The outer row with 60 equally spaced holes was used for low speed counting and the inner row with 12 equally spaced holes was used for high speed counting. A stroboscope was not suitable for the low speed range of 100 rpm. The number of holes scanned by the LDR was displayed on an oscilloscope.

e. Depth of Cut

One dial gage was mounted on a magnetic block which was attached to the base of the apparatus (Fig. 3.3.2). The undeformed surface was used as a reference for zero-depth of cut. The distance which the block was moved

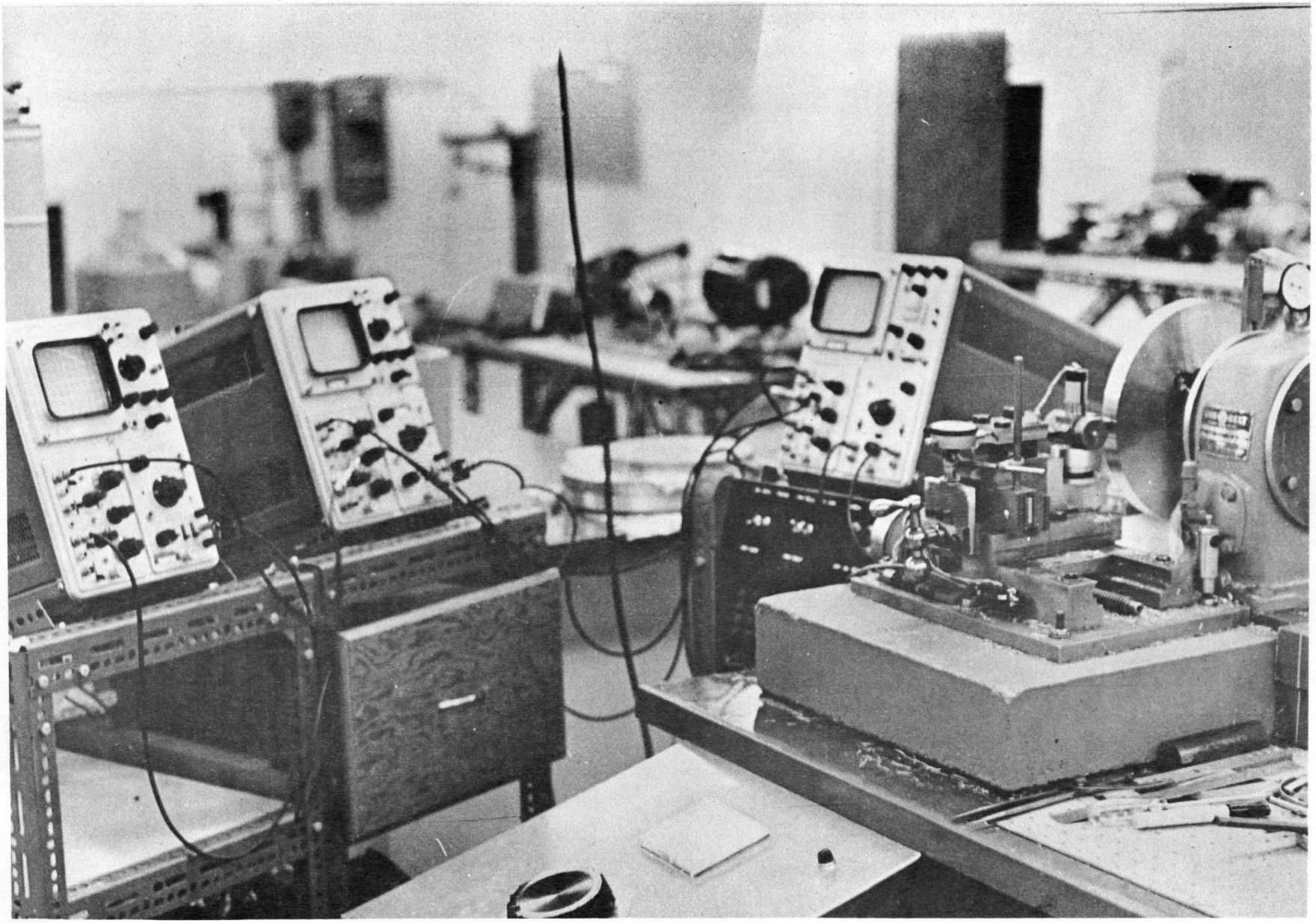

Fig. 3.3.2 General Arrangement of Apparatus and Instrumentation

into the groove of the workpiece was recorded as the depth of cut (see explanation in section 5.3, Test Procedure).

3.4 Recording System

The recording instruments included two model 564 and one model 564B Tektronic oscilloscopes. All had dual beam storage characteristics. The 564B was on the right (Fig. 3.3.2) and from right to left we numbered the oscilloscopes #1, #2, #3 for convenience. The displacement and acceleration signals were fed into channel 1 differential amplifier of the #1 oscilloscope, the displacement signal was fed into channel 2, and the velocity signal was fed into the horizontal display amplifier. #2 oscilloscope was used to record displacement and surface speed on a time base and #3 was used to record acceleration and velocity versus time. The arrangement could easily be altered if a different combination of variables on each oscilloscope was desired. The calibration of these signals is shown in Appendix II.

In addition to recording of various signals, the recording system of Fig. 3.3.1 was designed to achieve two objectives. The first was to record data at the same distance from the starting point. A groove was filed for the start of cut as shown in Fig. 3.7.1. The tool bit was fed in to a prescribed depth and the recording system was triggered at the same distance from the groove along the periphery. This method minimized the inconsistency arising from the initial impact of the workpiece against the tool. The second objective was to obtain a single phase-plane plot on #1 scope [17] and a single-sweep triggering of the other two scopes. The storage

oscilloscopes did not provide a 'built-in' means of obtaining this type of display and an undesired continuous trace appeared on the screens. In order to overcome this difficulty the one-cycle sequence triggering system of Fig. 3.3.3 was developed. In addition, a modification to the tube beam blanking circuit was necessary. The purpose of the triggering system was to unblank and blank the storage tube beam at the desired instant of time.

3.4.1 Spot Triggering Unit [17]

A light discriminating resistor (LDR) was used for the spot triggering. Each time a shield, which could be adjusted to any desired position around the circumference of the workpiece, moved between the light beam and the LDR it activated a relay which triggered the specially designed sequence circuit of Fig. 3.3.3. The sequence trigger permitted a single x-$\dot{x}$ phase plane display on #1 screen. Provision was made also to utilize the sequence circuit for activating the single sweep triggers of the #2 and #3 oscilloscopes thus ensuring synchronous recording when a comparison between various combinations such as cutting force-surface speed or cutting force-time traces, were required during one cycle of vibration.

3.4.2 One Cycle Sequence Triggering System [17]

The one cycle sequence triggering system used the displacement signal produced by the strain gauges in the cantilever beam. It was important that switching load effects from the triggering system did not influence the displacement signals being received and recorded. A vacuum tube d. c.

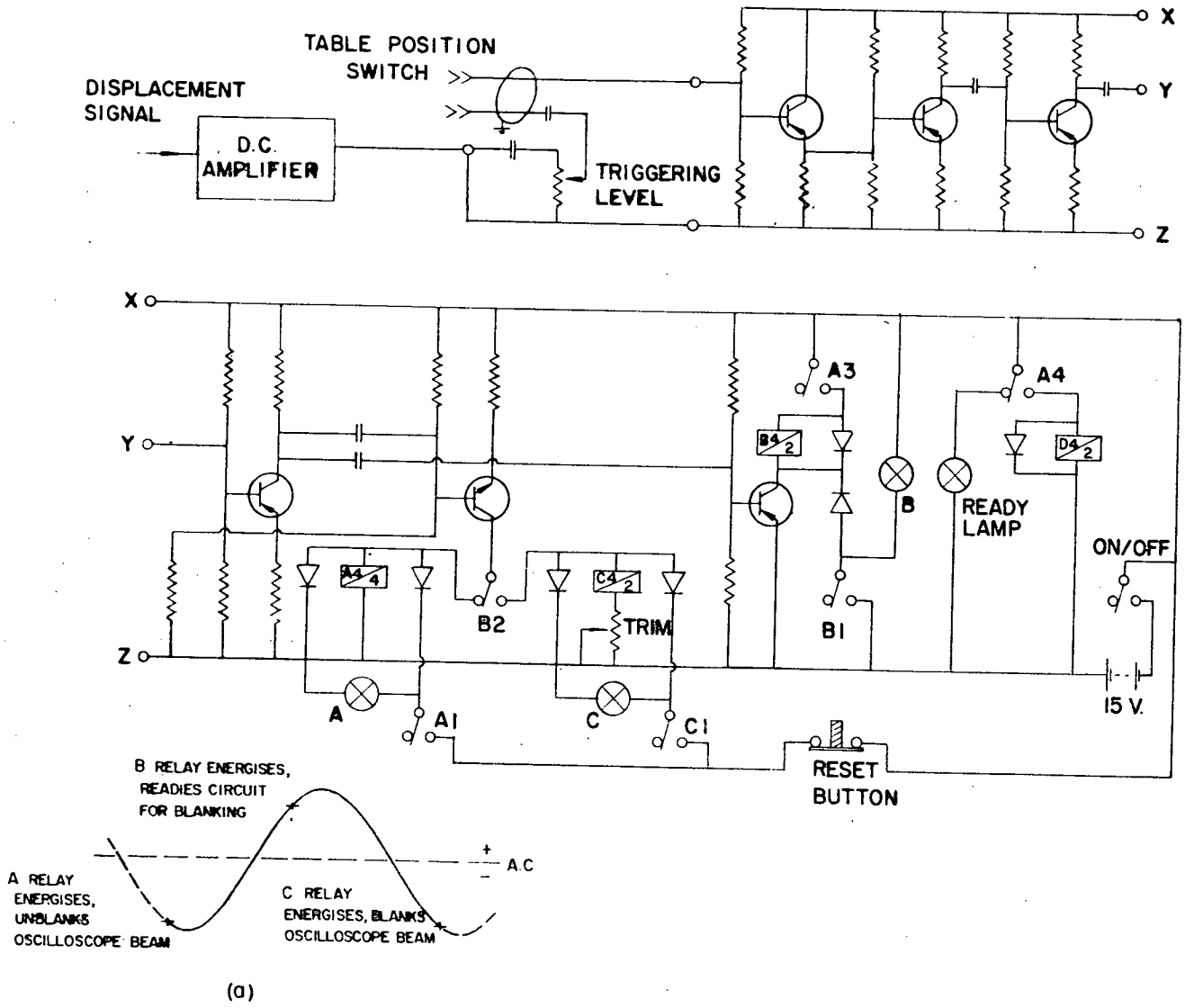

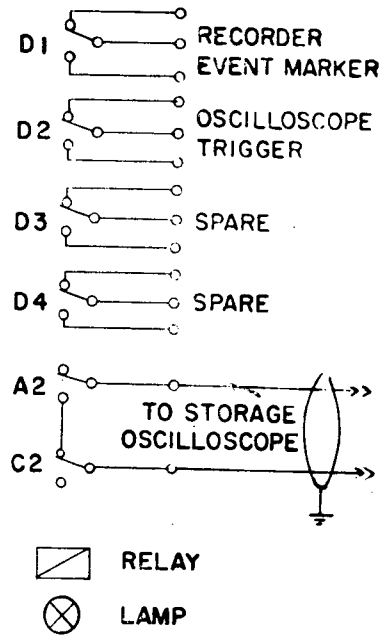

Fig. 3.3.3 One Cycle Sequence Trigger Circuit [17]

amplifier and a 10-megohm input impedance before the triggering unit eliminated switching load effect. The output impedance of this amplifier had a low value and was well suited to the input impedance of the triggering unit.

The essential parts of the sequence circuit consisted of three relays which were activated by the displacement signal. The negative electrical displacement signals were chosen as the start point. To obtain a one cycle display also meant that the negative displacement signals must also serve as an end point signal. It was necessary therefore to interlock this switching circuit so that the start and end point relays could neither operate simultaneously nor operate to closure before start. Fig. 3.3.3(a) shows a diagram of the signal. The use of a third relay to the system provided the means of sequencing events to the desired operation. The additional relay was energized by the positive electrical displacement signal and again had to be sequenced so that a negative start signal had to occur before this relay would energize. A fourth relay provided means for synchronizing triggering of the switching of the recording instruments.

The amplitude of the electrical displacement was not constant and was dependent on the degree of displacement of the cantilever beam. It was therefore necessary to provided variable controls for adjusting the electrical signals in the triggering unit so as to encompass the varying signal levels thereby ensuring relay closure. Electrical noise had to be eliminated so as to prevent accidental triggering of the unit.

3.5 Cutting Tool Selection

The cutting tool was selected according to three criteria :

(1) The tool bit had to remain sharp throughout the process of experiment to eliminate the effect of amplitude change due to tool wear [3].

(2) Side thrust on the tool had to be minimized to reduce horizontal vibration.

(3) The amplitude of vibration had to be sufficiently large compared to the noise level of the recording instruments.

For the cantilever beam used (0.2"×1"), it was observed that for cutters with less than 20°rake, the workpiece disc tended to seize the cutting tool after a short period of violent chatter. Feeding along the direction of the axis of the disc with pointed tool bit was tried, but the effects of regeneration were obvious. It was decided to adopt the tool bit of the geometry as shown in Fig. 3.5.1.

The tool bit had to be sufficiently ductile to prevent breakage during chatter. Tungsten carbide, a strong wear-resisteant but brittle material, was tried but found to be unsatisfactory for chatter experiments. High speed steel was sufficiently ductile hence it was selected.

3.6 Specimen

The material used as the workpiece was 70-30 lead free brass (Appendix III). The material was comparatively soft and tool wear was minimized. The chips produced were continuous and so effects produced by

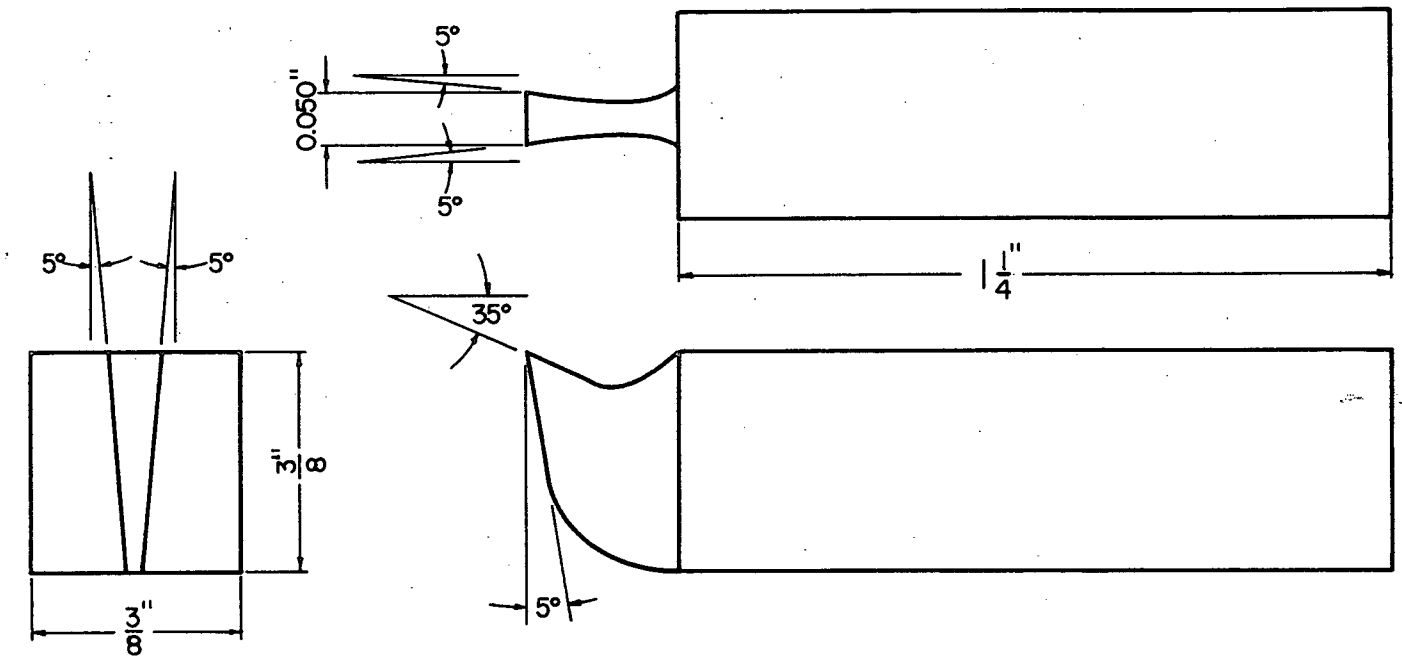

Fig. 3.5.1 Geometry of Tool Tip

breaking away of chips did not exist.

Leaded brass produces segmental or discontinuous chips due to the existence of globules of free lead in the metallurgical structure. These free lead particles are soft and weak, and during machining they cause the formation of a weak, brittle chip which does not build up on the tool. However, the lead does decrease the friction between the tool and the work. Lead free brass, on the other hand, is a homogeneous solid solution and produces continuous chips [20].

3.7 Experimental Method

3.7.1 Preliminary Investigation of System

Tests were conducted to study the effects of various parameters; these included surface speed, depth of cut and different cutting tools. The influence of the stiffness of supporting system was investigated in the early stages of the research. It was found that a 0.2 in thick by 1 in deep beam permitted the application of sufficiently high cutting forces but the displacement was still low enough so as to give insignificant curvature effects. Two lead weights were added to reduce the natural frequency. The vibrating system had an equivalent mass of 0.923 lbm. The equivalent beam stiffness at the tool bit was 855.6 lb/in and the viscous damping coefficient was in the region of 0.008 lb/in/sec. The damping coefficient of the cutting system was obtained by performing a damped free vibration test with the tool bit clear of the workpiece. A displacement-time curve was obtained

from such a test and the coefficient was calculated by the logarithmic decrement method (Appendix I). The system damping could also be obtained from the $(m\ddot{x} + kx)$ versus $\dot{x}$ trace obtained during free vibration. The damping coefficient was obtained directly from the slope of the trace.

A damped natural frequency of 95 Hz was found for the supporting system. The small amount of system damping gave a natural frequency which was virtually the same as the undamped case. The calibration of the beam stiffness and the system natural frequency is described in Appendix I.

3.7.2 Specimen Preparation

A freshly trued surface had to be used for each run of the experiment since the effects of regeneration were undesirable. During preliminary trials, the workpiece was tried in a commercial lathe. However, great difficulty was experimenced in obtaining alignment when replacing the workpiece in the experimental apparatus. The problem was solved by turning the workpiece in situ with a stiff 3/4 in tool, clamped to the supporting block.

3.7.3 Test Procedure

The method of cutting is shown in Fig. 3.7.1. A groove of prescribed depth was filed across the trued surface of the workpiece. The cutting tool was then moved into the groove. Initial cutting was accomplished by rotating the speed reducer by hand. A continuous chip was formed.

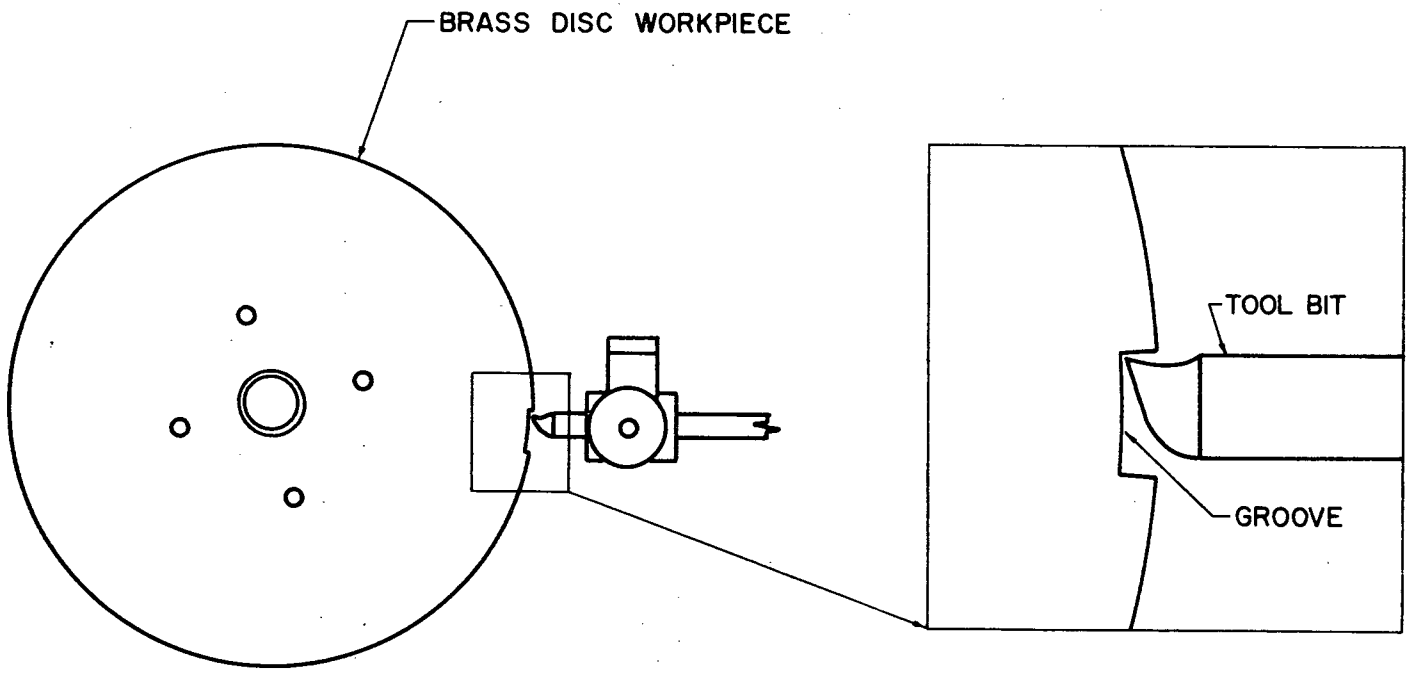

Fig. 3.7.1 Method of Cutting

The motor was started after the tool had completed a cut of about 1 in along the circumference. The setting of the index on the motor ammeter provided nominal control of the surface speed. The triggering of the recording systems was automatic and has been explained earlier. Poloroid photographs were taken of the oscilloscope storage for every run.

For each set of tests only one parameter was varied. Prior to each test, the cantilever beam was set at its natural position and all instruments were checked for reference level.

CHAPTER IV

4.1 Graphical Construction of Phase Plane

A typical phase plane during one cycle of chatter vibration is shown in Fig. 4.1.1 (a). Displacement and acceleration signals are shown in Fig. 4.1.1 (b). Displacement and velocity signals are shown in Fig. 4.1.1 (c). These photographs were taken on three storage oscilloscopes which were triggered at the same instant as explained previously. Additional examples of the phase plane and x, $\dot{x}$, $\ddot{x}$ signals are given in Fig. 4.1.2 (a), Fig. 4.1.2 (b) and Fig. 4.1.2 (c).

If the displacement, velocity and acceleration signals recorded in Fig. 4.1.1 (b) and Fig. 4.1.1 (c) were plotted on graph paper, a force curve for each variable is obtained as $F(x)$, $F(\dot{x})$ and $F(\ddot{x})$, (Fig. 4.1.3 (a), Fig. 4.1.3 (b) and Fig. 4.1.3 (c)) where

$$F(x) = kx \; ; \qquad F(\dot{x}) = r\dot{x} \; ; \qquad F(\ddot{x}) = m\ddot{x} \; .$$

Instead of using real time as the abscissa, the angular displacement of the tool bit was used. When cutting was commenced, the tool was deflected and began to vibrate around a neutral position. This neutral position is used as a position of zero angular displacement. Summing these forces, the desired cutting force curve is obtained (Fig. 4.1.4). For the purpose of graphical construction, a $\frac{F - r\dot{x}}{\sqrt{km}}$ versus θ is also required. Since

$$F - r\dot{x} = m\ddot{x} + kx \; ,$$

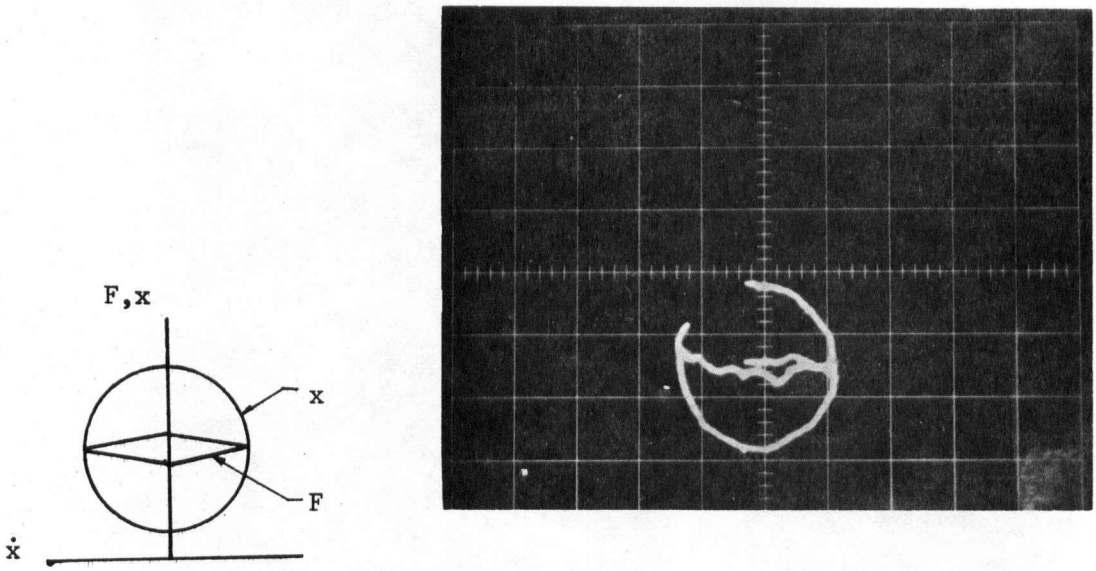

Scale : Force 1 Div = 1.7 lb

Displacement 1 Div = 0.002 in

Velocity 1 Div = 1.29 in/sec.

Fig. 4.1.1 (a) Recorded Phase Plane Diagram

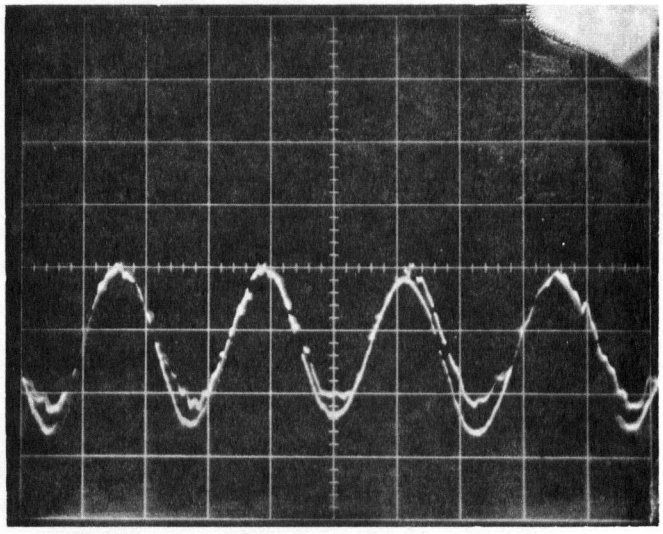

acceleration 1 Div = 0.002 in

Fig. 4.1.1 (b) Recorded Displacement and Velocity Signals

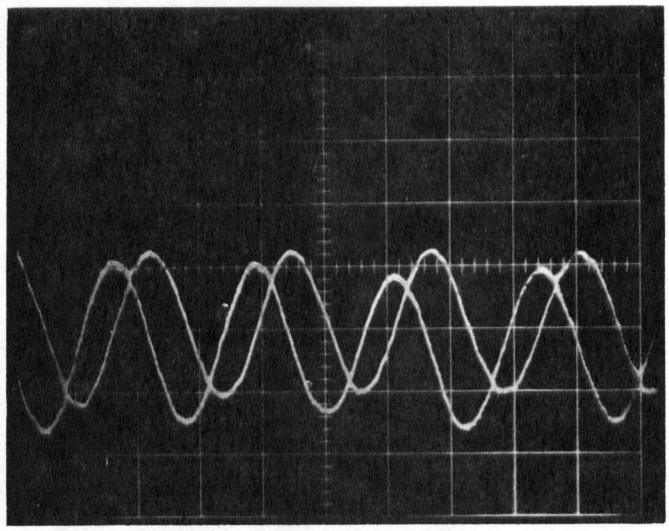

Upper curve - Velocity 1 Div = 1.29 in/sec
Lower curve - displacement 1 Div = 1.85 g.

Fig. 4.1.1 (c) Recorded Displacement and Accel ration Signals

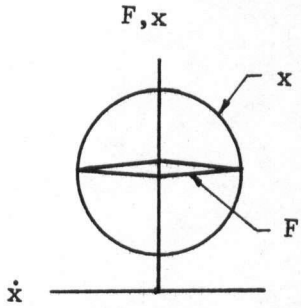

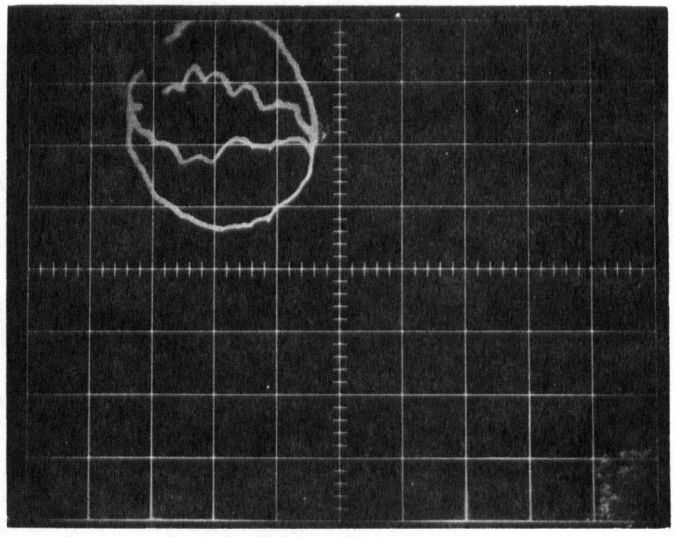

Scale : Force 1 Div = 1.7 lb
Displacement 1 Div = 0.002 in
Velocity 1 Div = 1.29 in/sec

Fig. 4.1.2 (a) Recorded Phase Plane Diagram

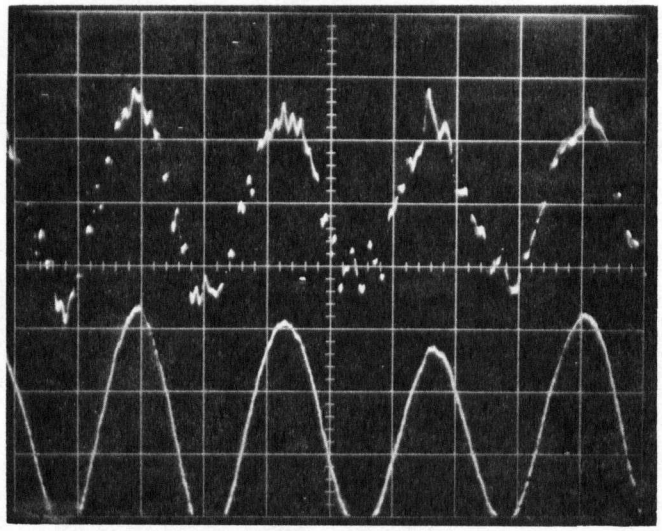

Smooth curve - Displacement 1 Div = 0.002 in
Broken curve - acceleration 1 Div = 1.85 g.

Fig. 4.1.2 (b) Recorded Displacement and Velocity Signals

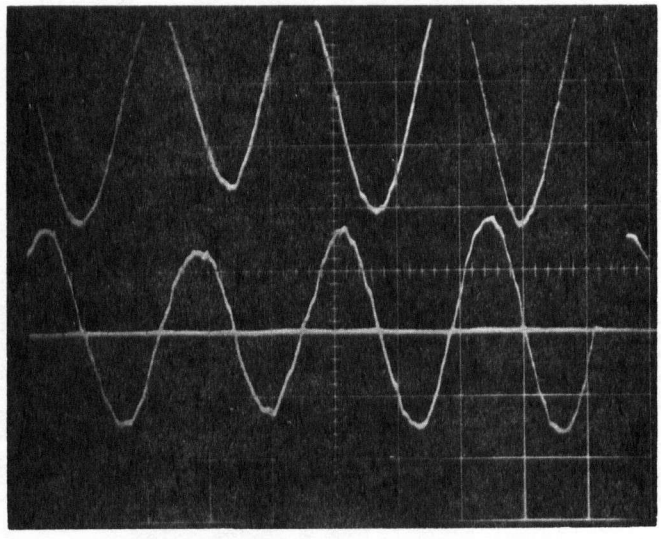

Upper curve - displacement 1 Div = 0.002 in
Lower curve - Velocity 1 Div = 1.29 in/sec

Fig. 4.1.2 (c) Recorded Displacement and Acceleration Signals

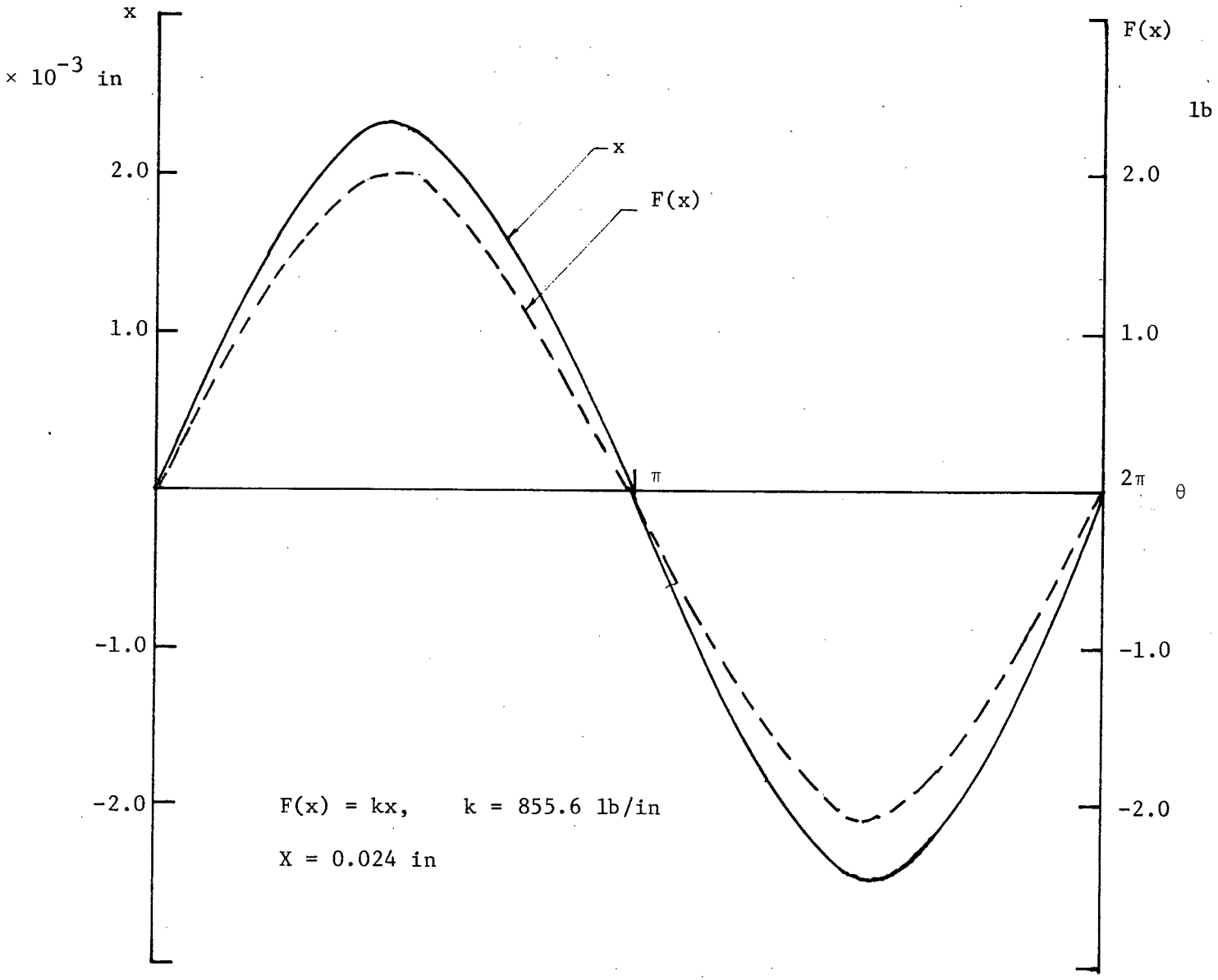

Fig. 4.1.3 (a) Displacement versus Angular Displacement

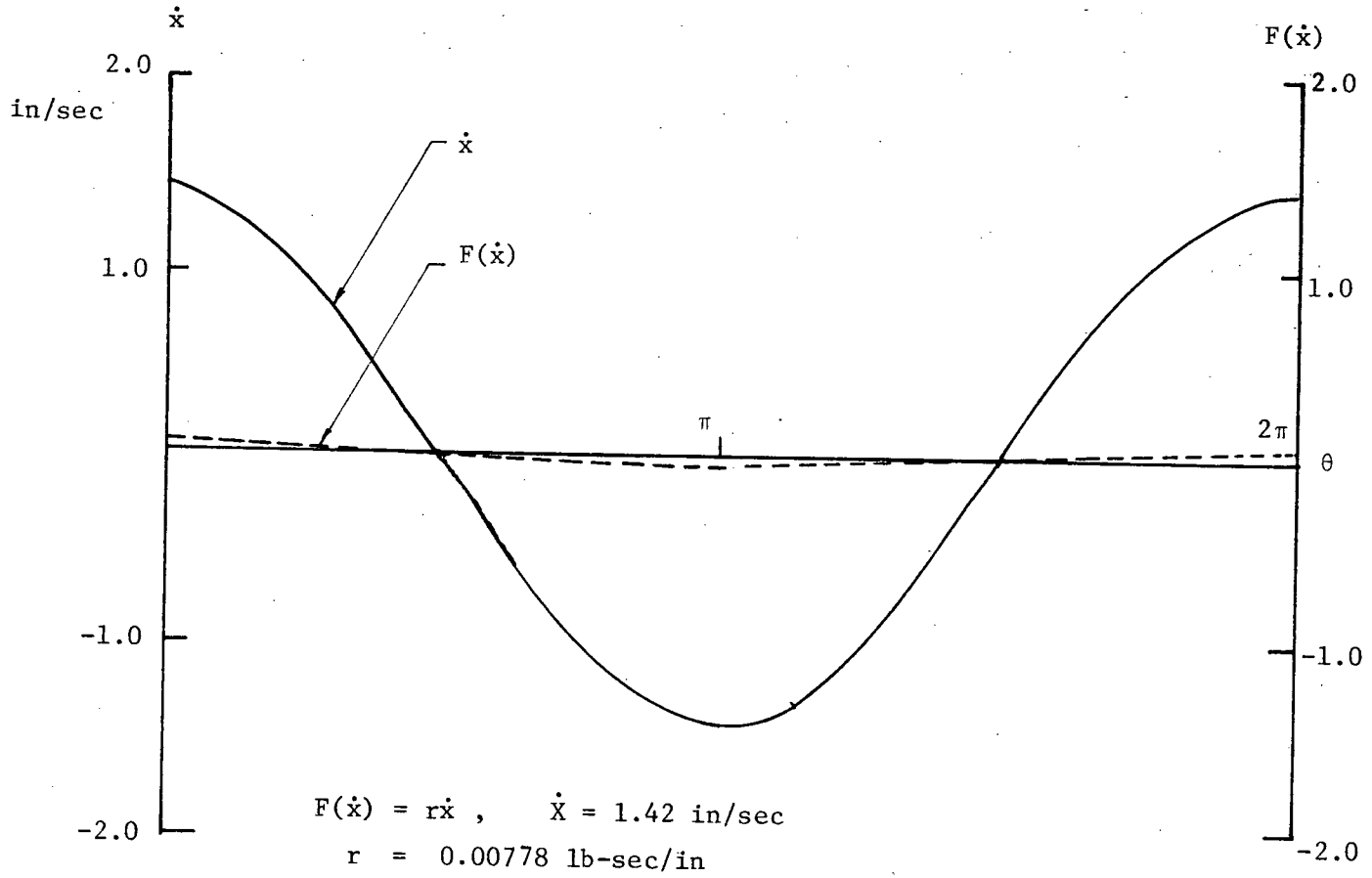

Fig. 4.1.3 (b) Velocity versus Angular Displacement

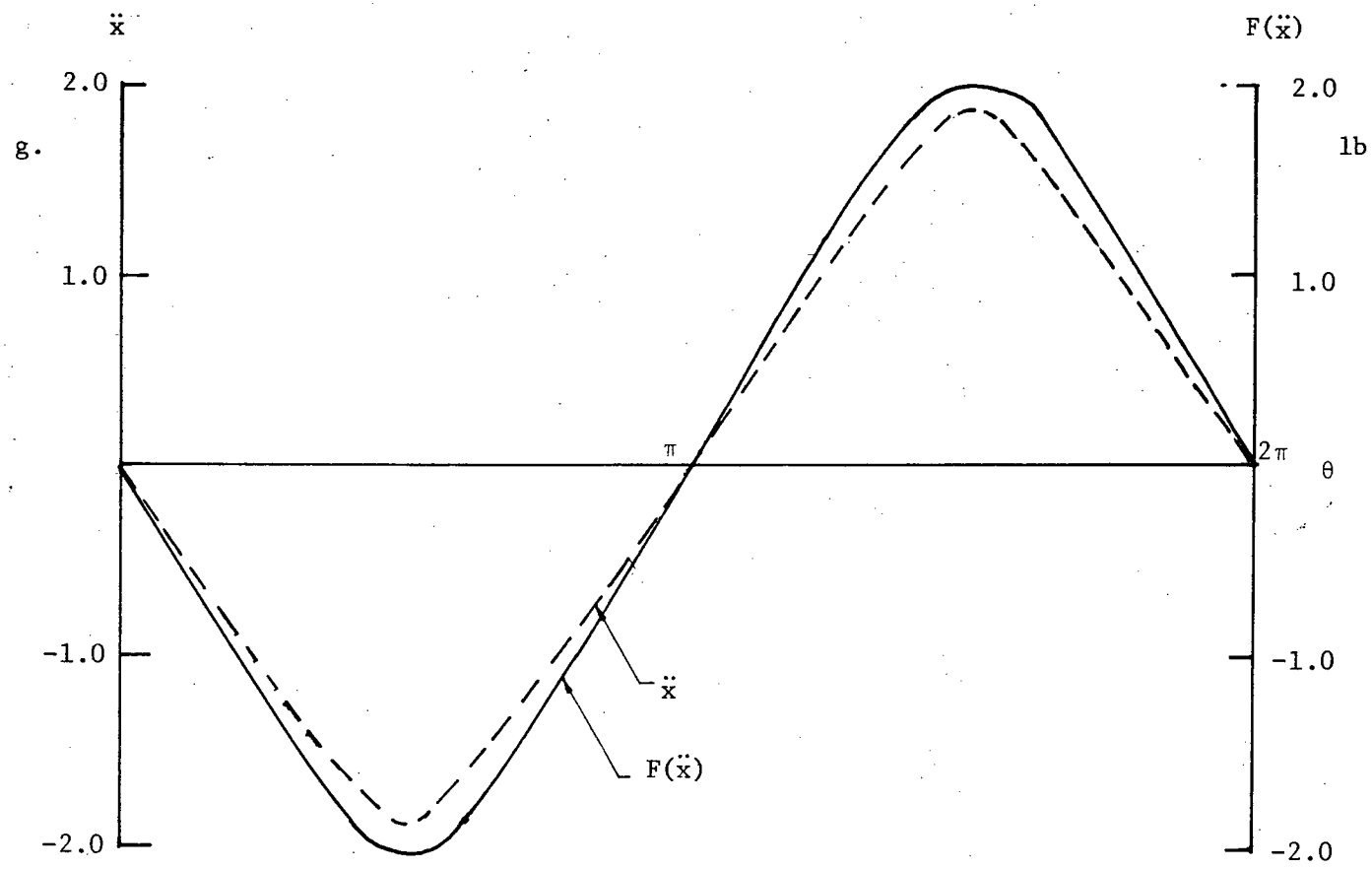

$F(\ddot{x}) = m\ddot{x}$; $m = 0.923$ lbm

$\ddot{X} = 2.04$ g.

Fig. 4.1.3 (c) Acceleration versus Angular Displacement

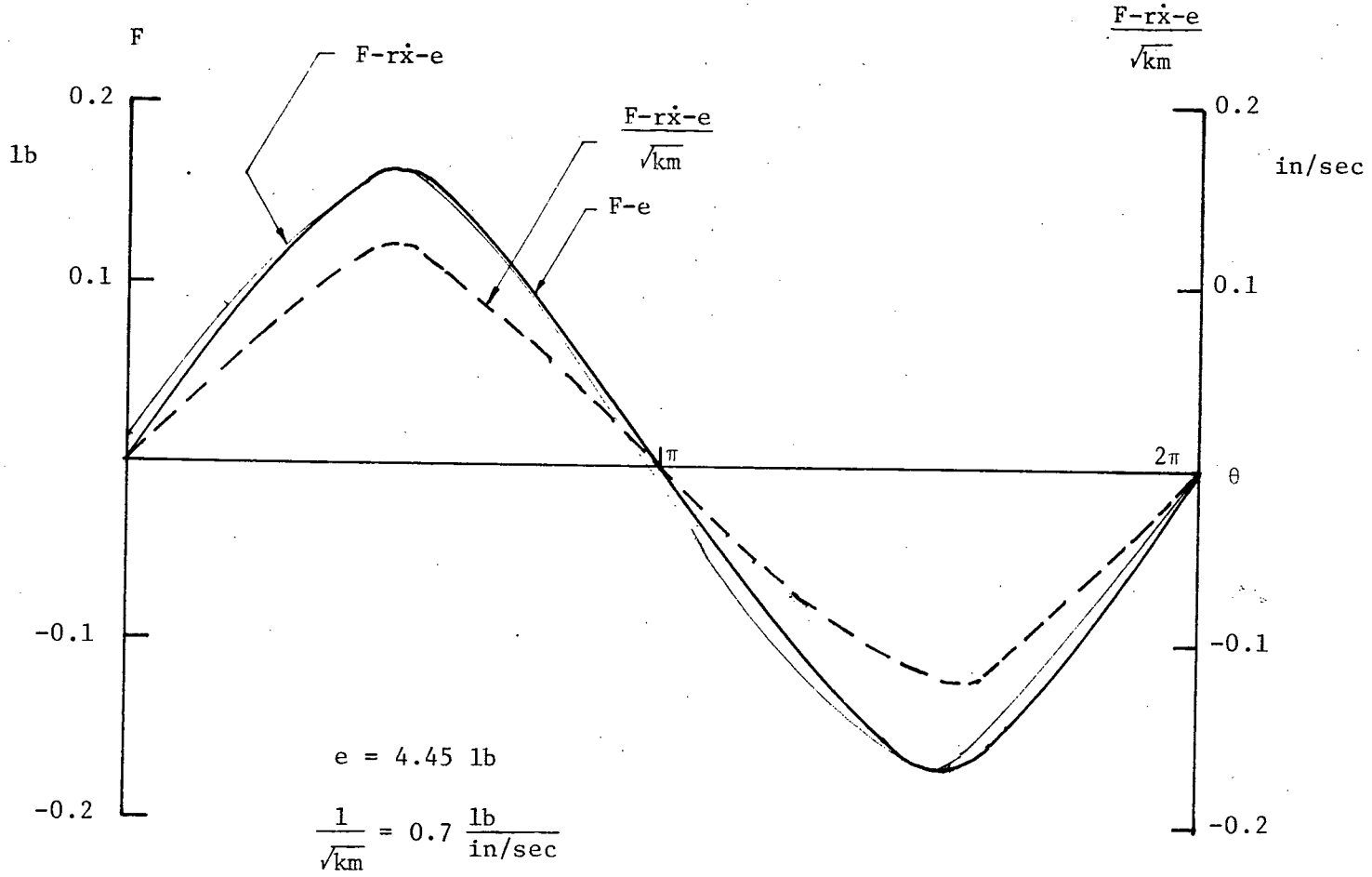

Fig. 4.1.4 Dynamic Cutting Force versus Angular Displacement

the curve was obtained by adding $F(\ddot{x})$ to $F(x)$ and then multiplied by the constant factor $\frac{1}{\sqrt{km}}$. This curve was transformed onto a phase plane. The procedure of graphical construction of the phase plane from the force curve as explained in section 2.4 then follows. The result is shown in Fig. 4.1.5. The constructed phase plane was in excellent agreement with the experimental recording.

4.2 Vibration Amplitude and Frequency

Preliminary investigation had indicated that vibration amplitude grows with increasing surface speed up to a critical speed. The vibration then became unstable and decayed upon further increase in speed. Test results for the present system have been shown that the critical speed to be about 7 in/sec for three different depths of cut (Fig. 4.2.1 (a), Fig. 4.2.1 (b) and Fig. 4.2.1 (c)). The amplitude signals appear to be nearly sinusoidal with slight modulation.

The frequency of chatter vibration was stable in all tests (Fig. 4.2.2 (a), Fig. 4.2.2 (b) and Fig. 4.2.2 (c)). The average value was 100 Hz, 5 Hz higher than the damped natural frequency of the cantilever beam. This might suggest a net negative overall damping coefficient. Previous workers have obtained frequencies both higher and lower than the natural frequency [2, 23].

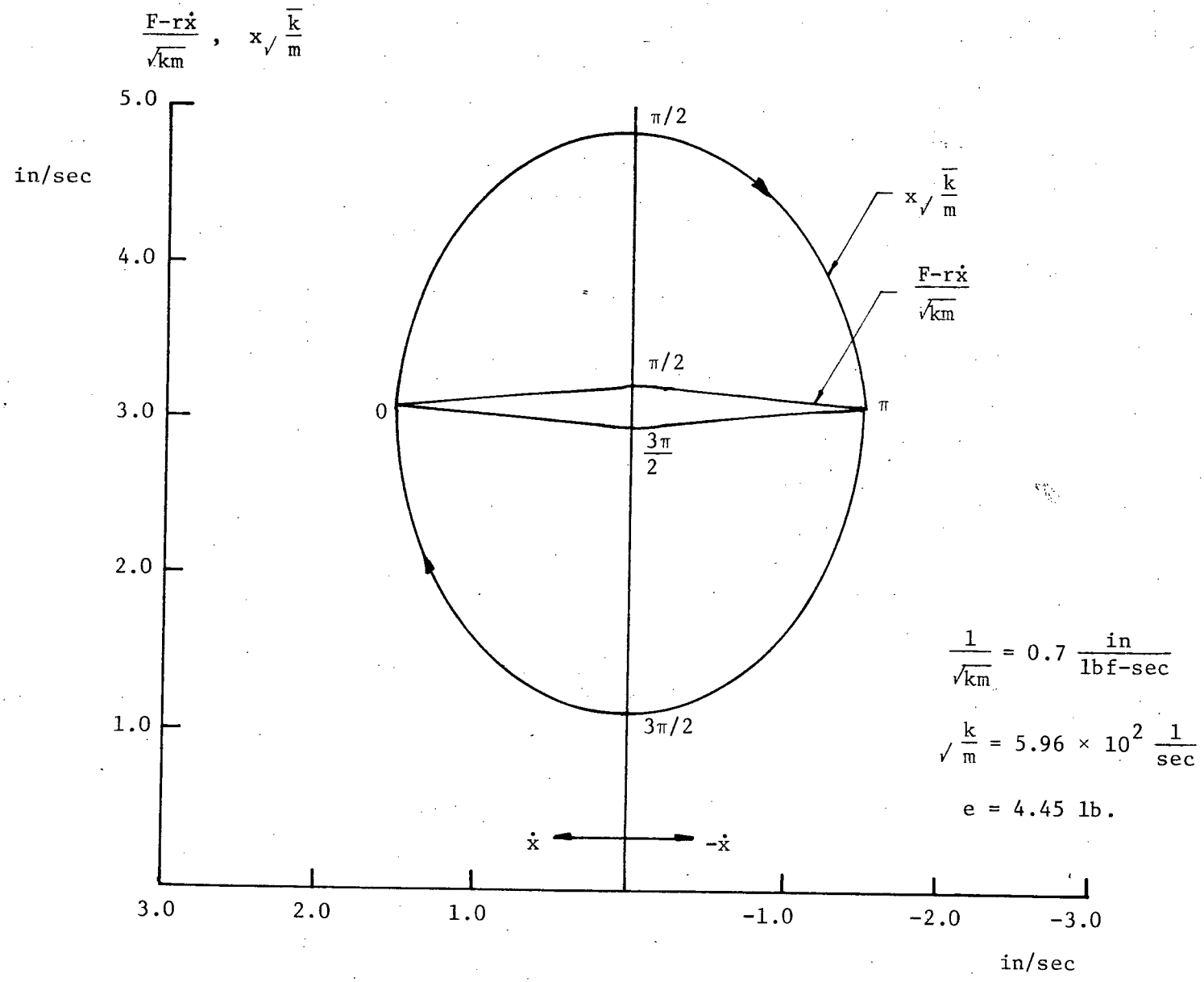

Fig. 4.1.5 Graphical Construction of Phase-Plane Diagram

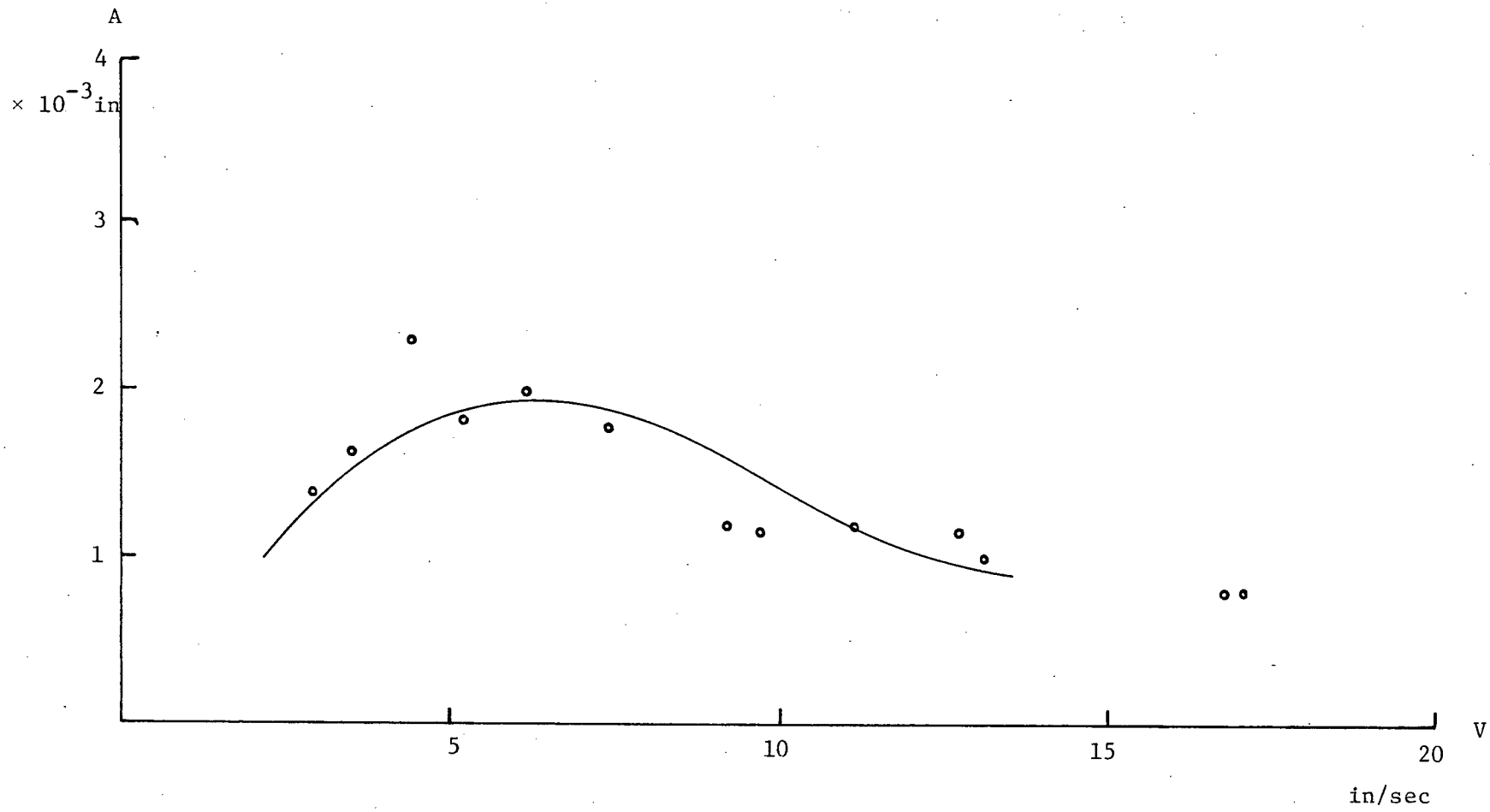

Fig. 4.2.1 (a) Amplitude of Vibration versus Surface Speed for $t_1 \approx 0.005$ in

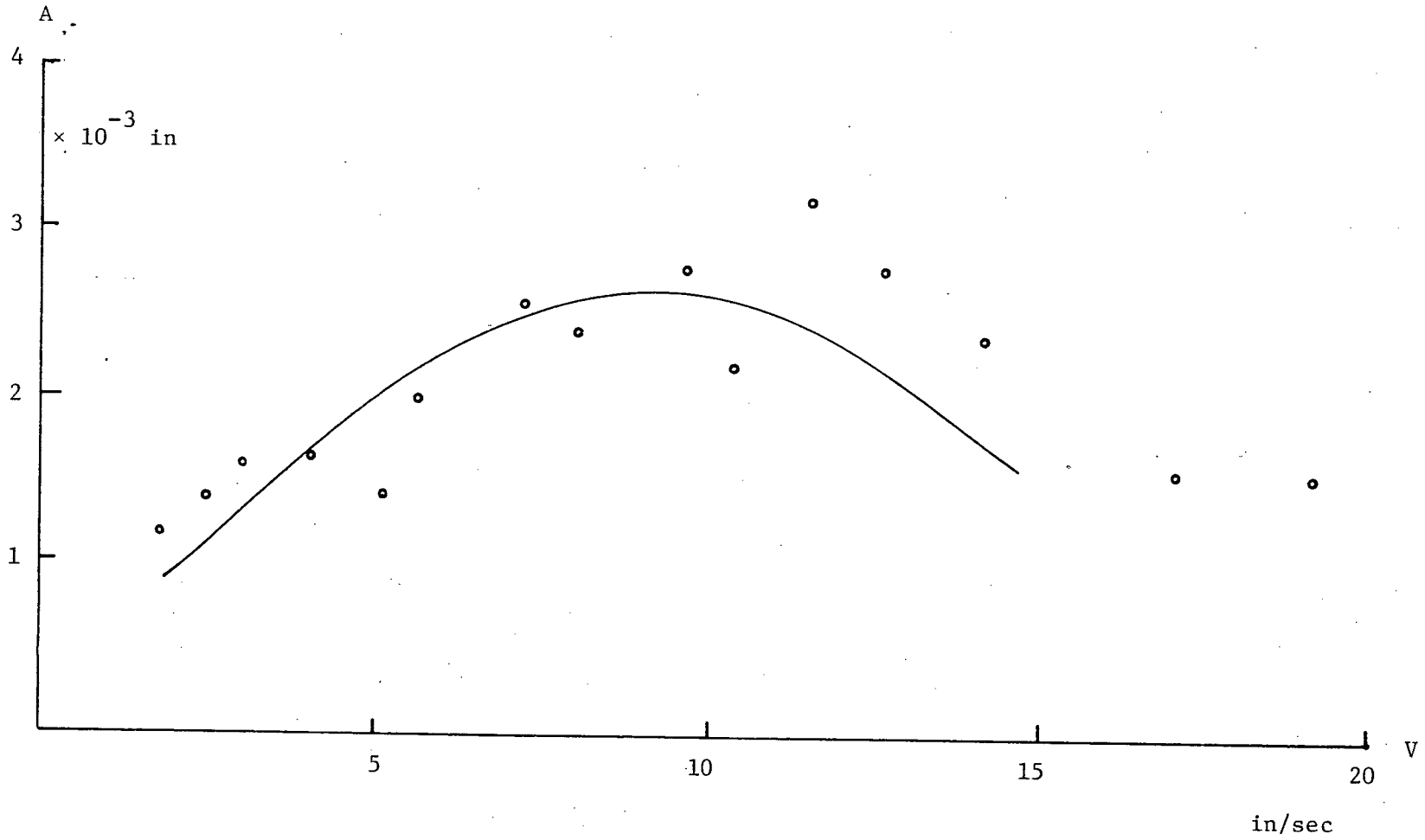

Fig. 4.2.1 (b) Amplitude of Vibration versus Surface Speed for $t_1 \cong 0.013$ in

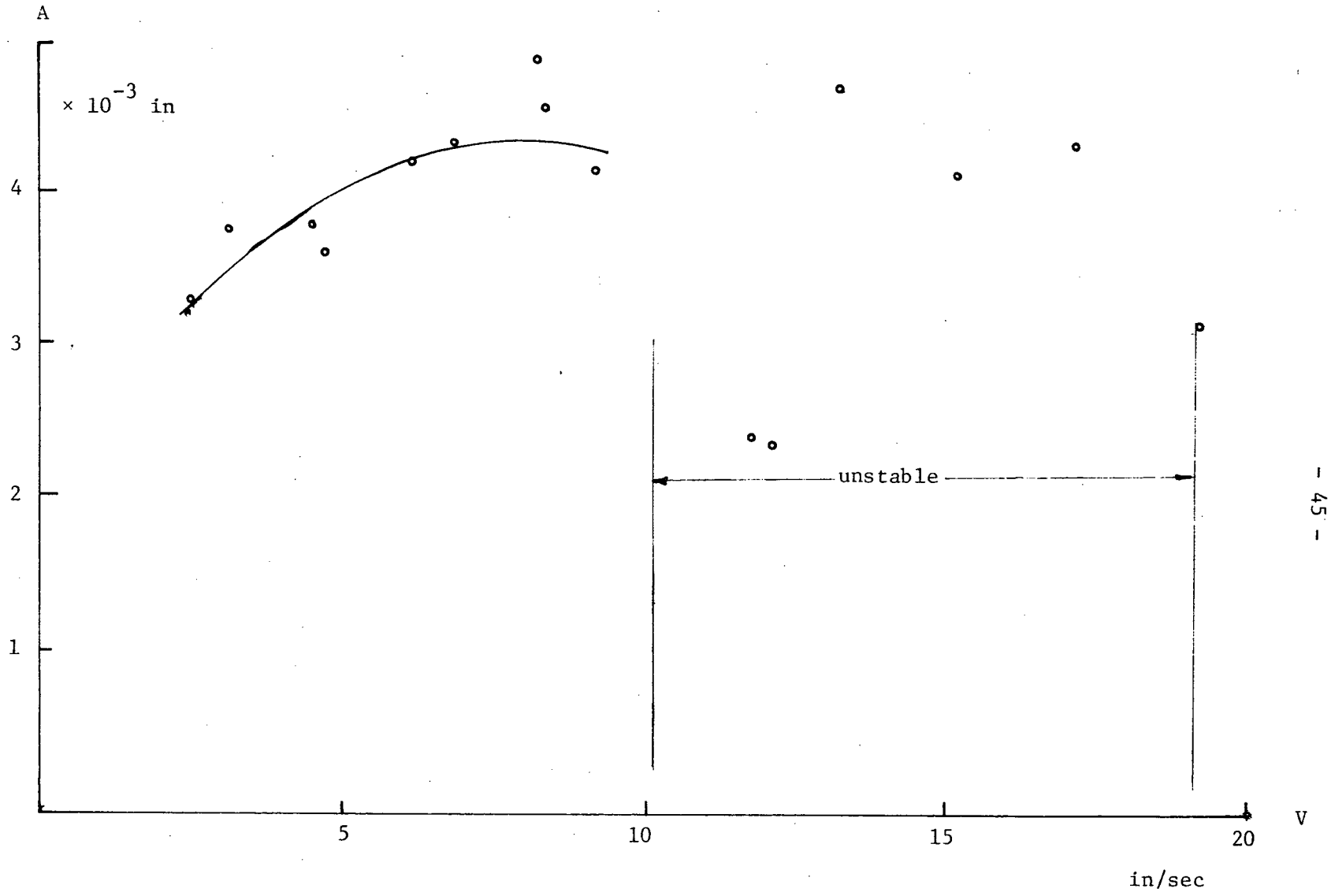

Fig. 4.2.1 (c) Amplitude of Vibration versus Surface Speed for $t_1 \cong 0.022$ in

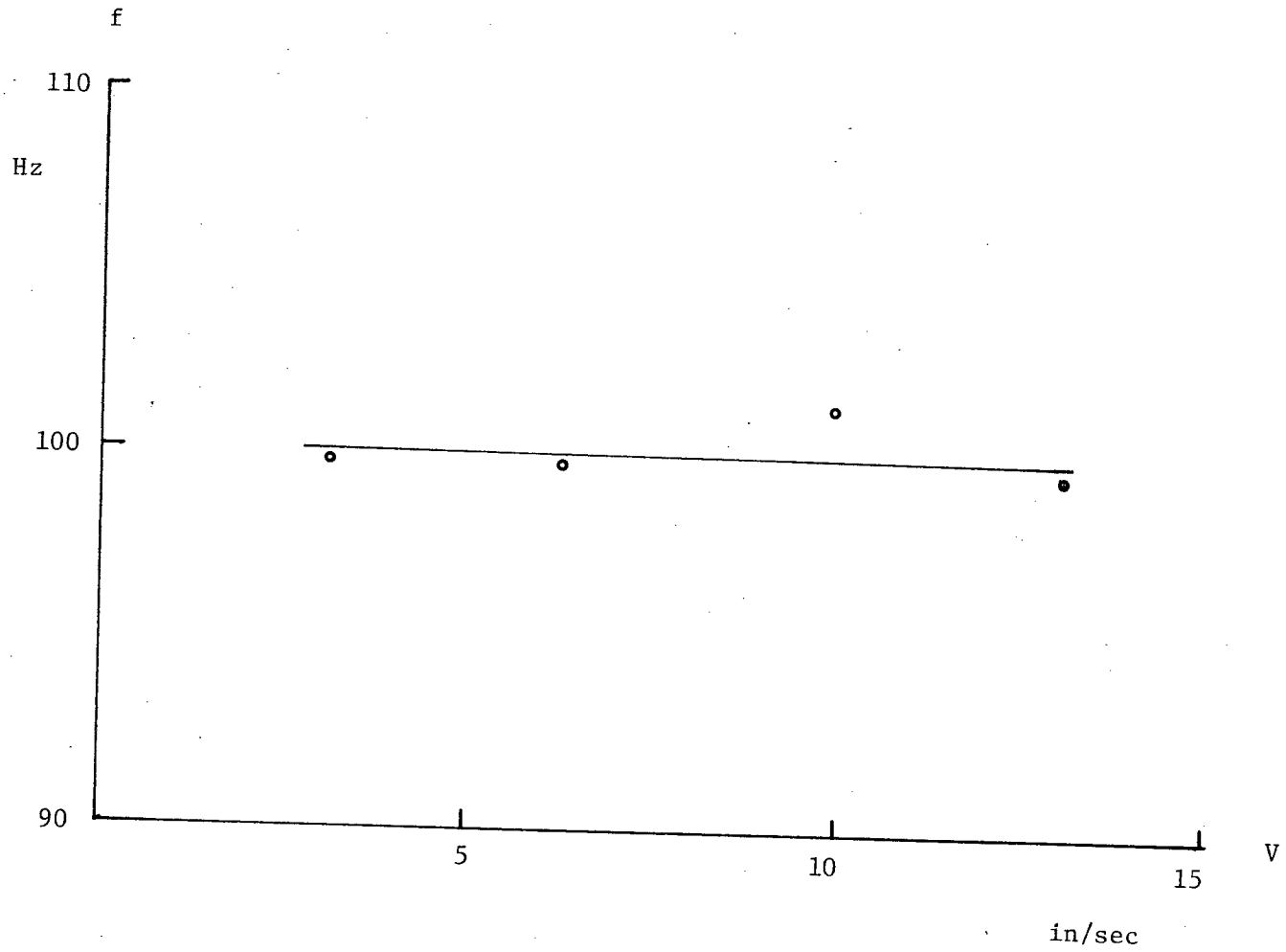

Fig. 4.2.2 (a) Cutting Frequency versus Surface Speed for $t_1 \cong 0.005$ in

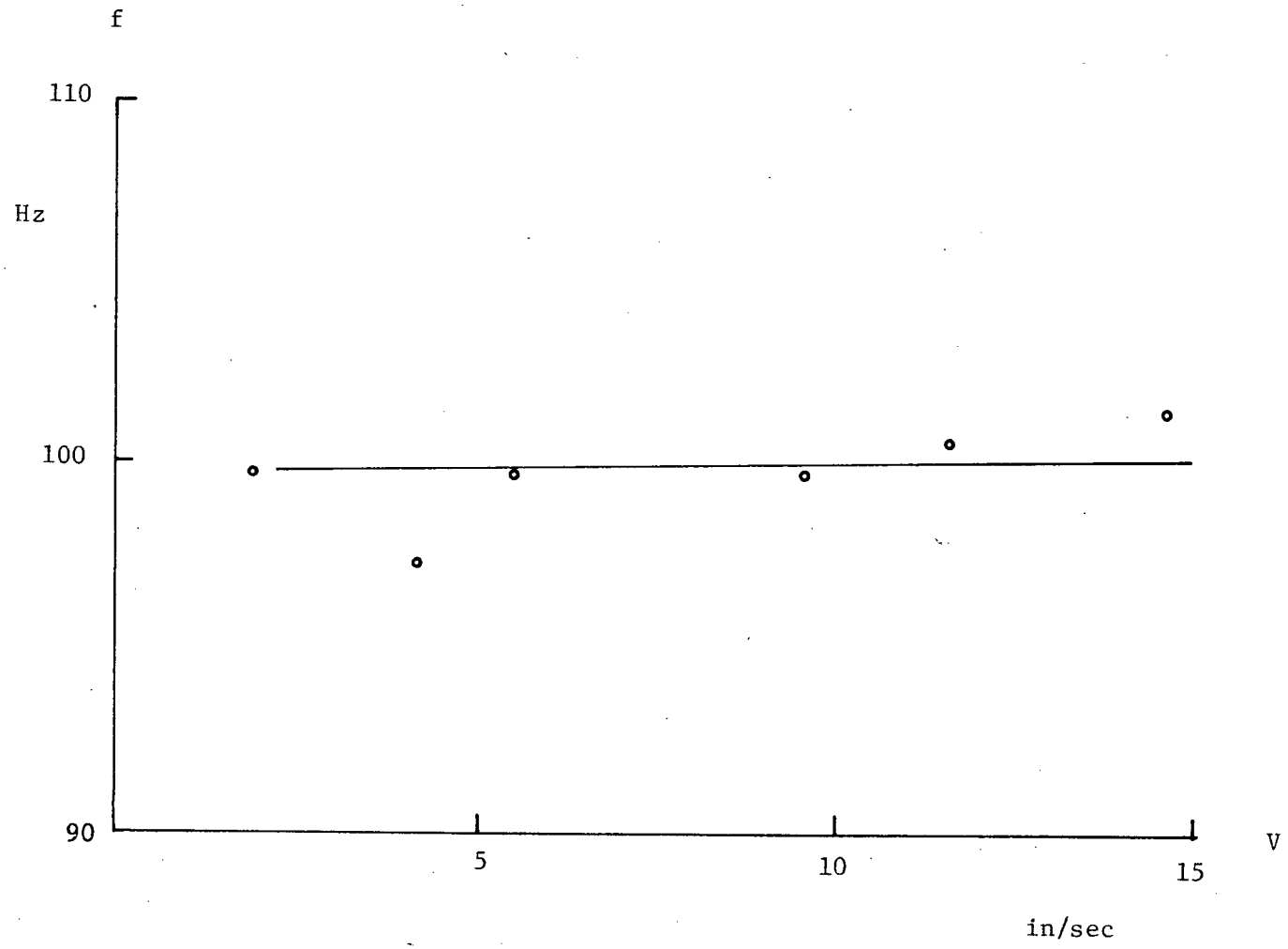

Fig. 4.2.2 (b) Cutting Frequency versus Surface Speed for $t_1 \cong 0.013$ in

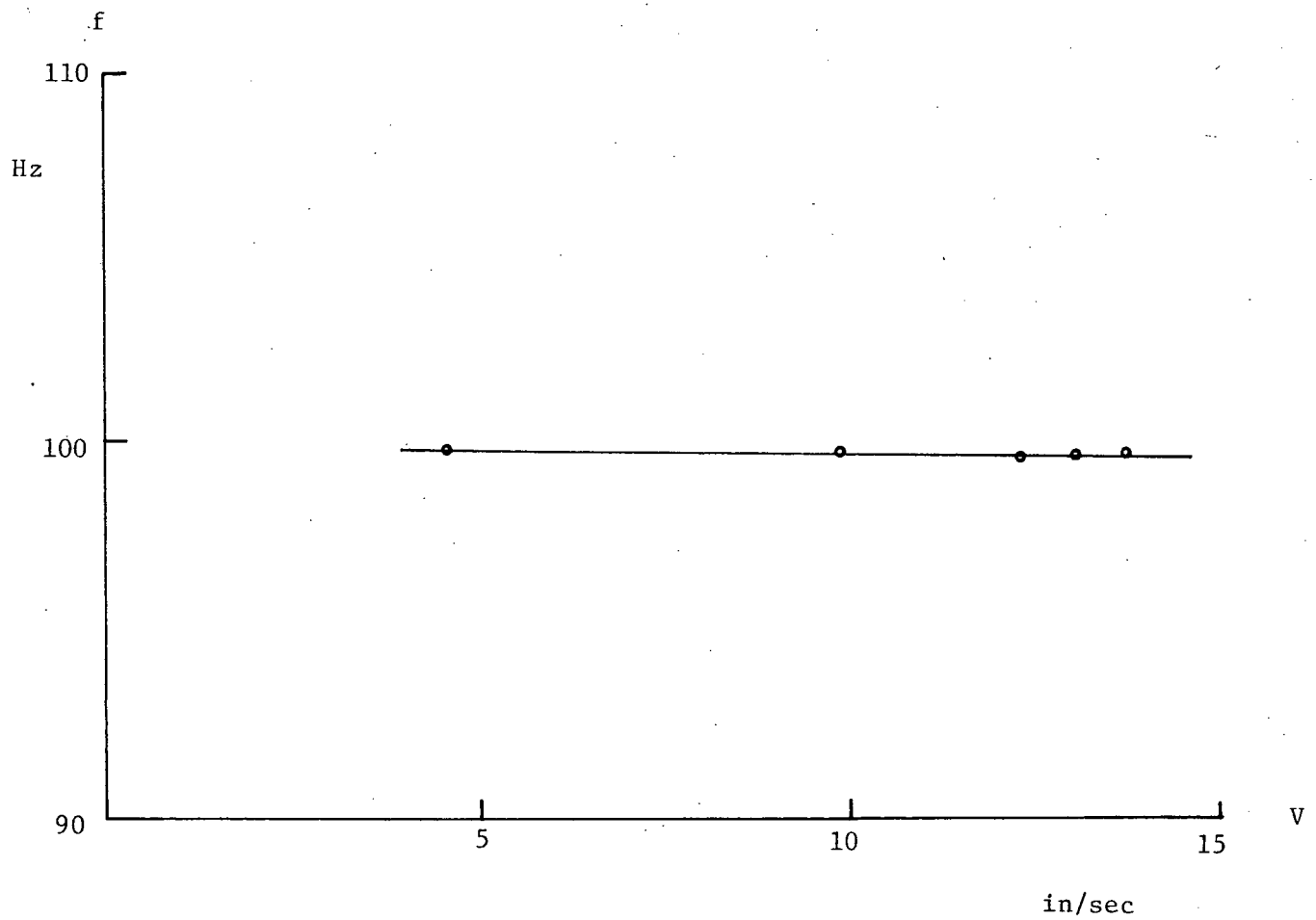

Fig. 4.2.2 (c) Cutting Frequency versus Surface Speed for $t_1 \cong 0.012$ in

4.3 Cutting Force

A dynamic cutting force-slip velocity curve is shown in Fig. 4.1.1 (a) and Fig. 4.1.2 (a). It is clear that, during one cycle of vibration, the cutting tool encountered both positive and negative force-velocity gradients. The simple, uniquely defined 'humped' curve observed by Ko [17] was not obtained. In most cases observed, a 'looped' force-velocity curve was recorded. The main difference may lay in the geometry of the two systems. In Ko's apparatus, a pin on disc arrangement, contact is maintained at constant load during vibration (Fig. 4.3.1). In the present apparatus, the normal forces acting on the tool face and tool flank are definitely functions of position.

Equation (5) can be written as :

$$m\ddot{x} + [r + f'(v) - \frac{1}{2}\dot{x}f''(v) + \frac{1}{6}\dot{x}^2 f'''(v)]\dot{x} + kx = e \ .$$

Since $m\ddot{x} + kx = F - r\dot{x}$, we have

$$[r + f'(v) - \frac{1}{2}\dot{x}f''(v) + \frac{1}{6}\dot{x}^2 f'''(v)] = \frac{[(F - r\dot{x}) - e]}{-\dot{x}}$$

which is the slope of the $(F - r\dot{x})$ curve on the phase plane diagram. The left hand side can be considered as the overall damping coefficient of the cutting system during chatter vibration. From the phase plane diagram, we can see that positive damping is encountered when the tool bit is moving away from the neutral position, thus restraining the amplitude growth. Negative damping is encountered when it moves towards the neutral position, thus providing energy to maintain the vibration. A force-displacement curve

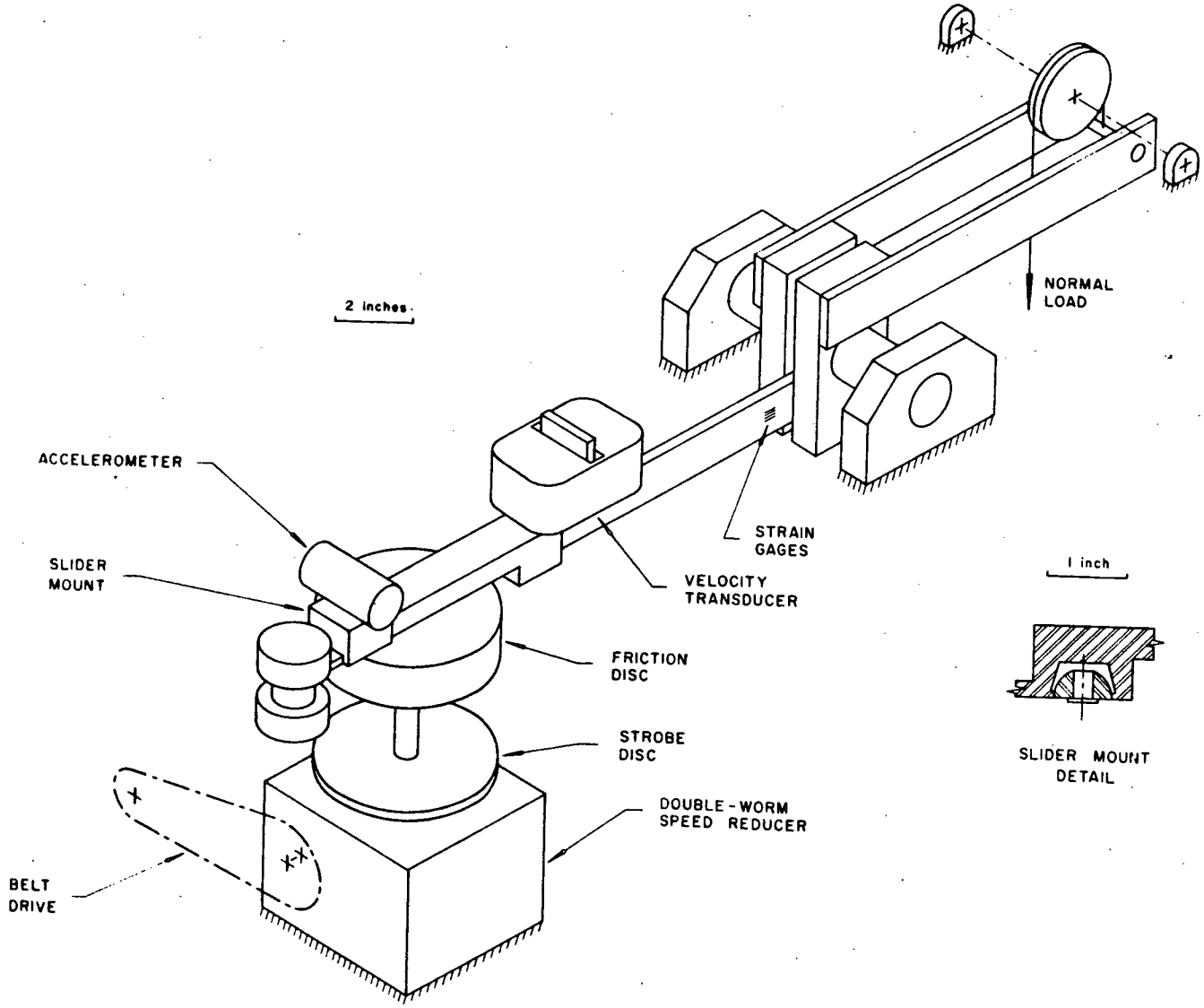

Fig. 4.3.1 Pin on Disc Friction Apparatus [17]

is shown in Fig. 4.3.2. The energy input into the system is dissipated by the structural damping.

The fact that the force-velocity curves are 'loop' shaped and closed at maximum and minimum absolute velocities may suggest acceleration and displacement signals are nearly sinusoidal and nearly 180 degrees out of phase. Thus, when $|f(x)| > |f(\ddot{x})|$, then $(m\ddot{x} + kx)$ varies in the same manner as the displacement signal. When transformed onto a phase plane, it becomes loop shaped.

The nominal cutting force versus surface speed curves (Fig. 4.3.3 (a), Fig. 4.3.3 (b) and Fig. 4.3.3 (c)) show a decreasing characteristic with increasing surface speed, which is in agreement with previous workers [3]. The cutting ratio curves (Fig. 4.3.4) are also in good agreement [11].

4.4 Frictional Experiment

A round-nosed pin was ground of high speed steel, the same material as the tool bit, and a series of experiments were carried out on the same apparatus. Only qualitative results could be obtained because there was no suitable means of measuring the normal force.

In Fig. 4.4.1, it can be seen that as the surface speed was increased from zero, stick-slip vibration commenced and its amplitude increased to a critical speed and then dropped to a low value. The phase plane became distinctly quasi-harmonic as the speed was further increased. The amplitude continued to grow until at about 7 in/sec it became unstable

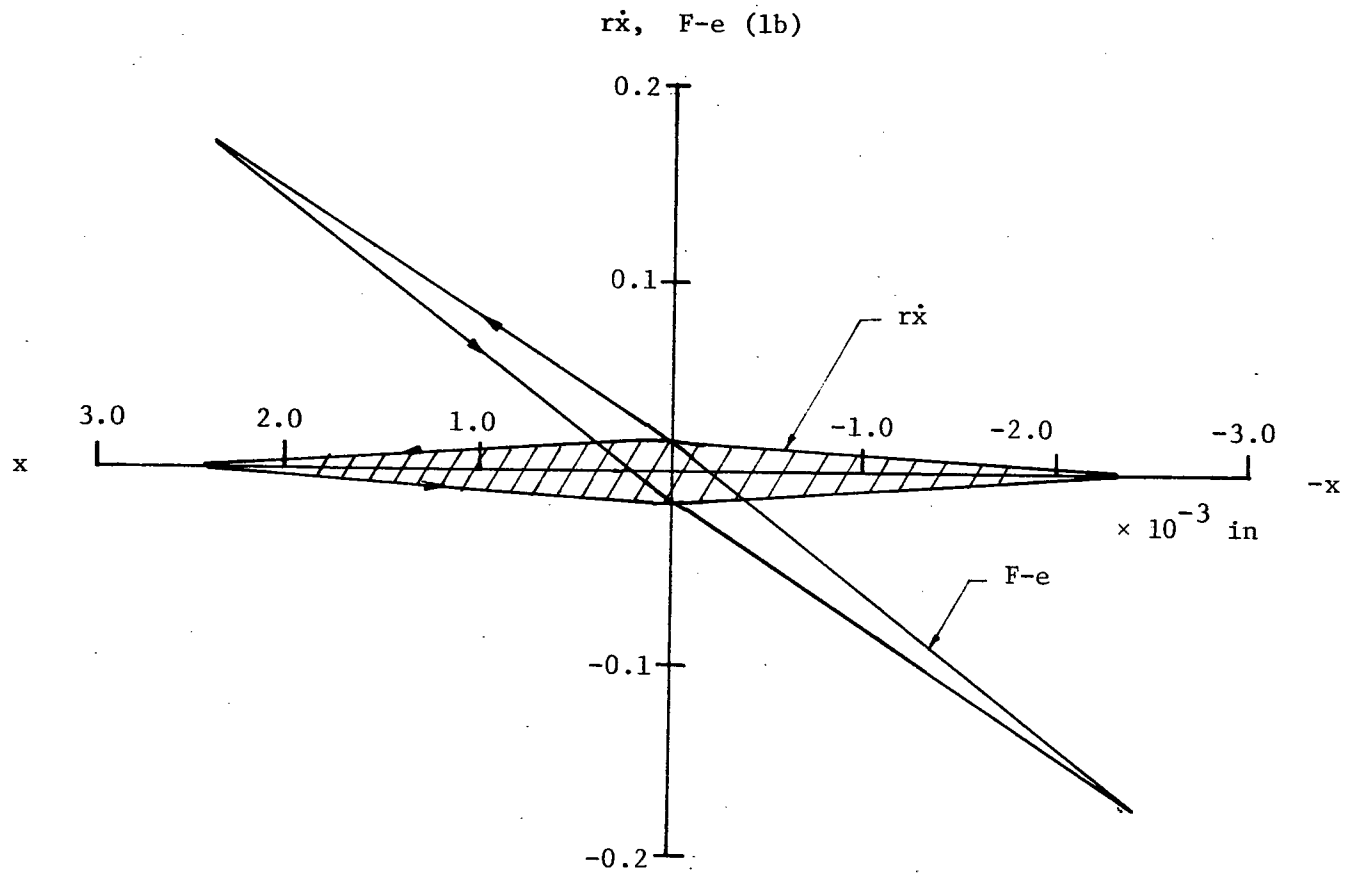

Fig. 4.3.2 Force versus Displacement during one cycle of Vibration

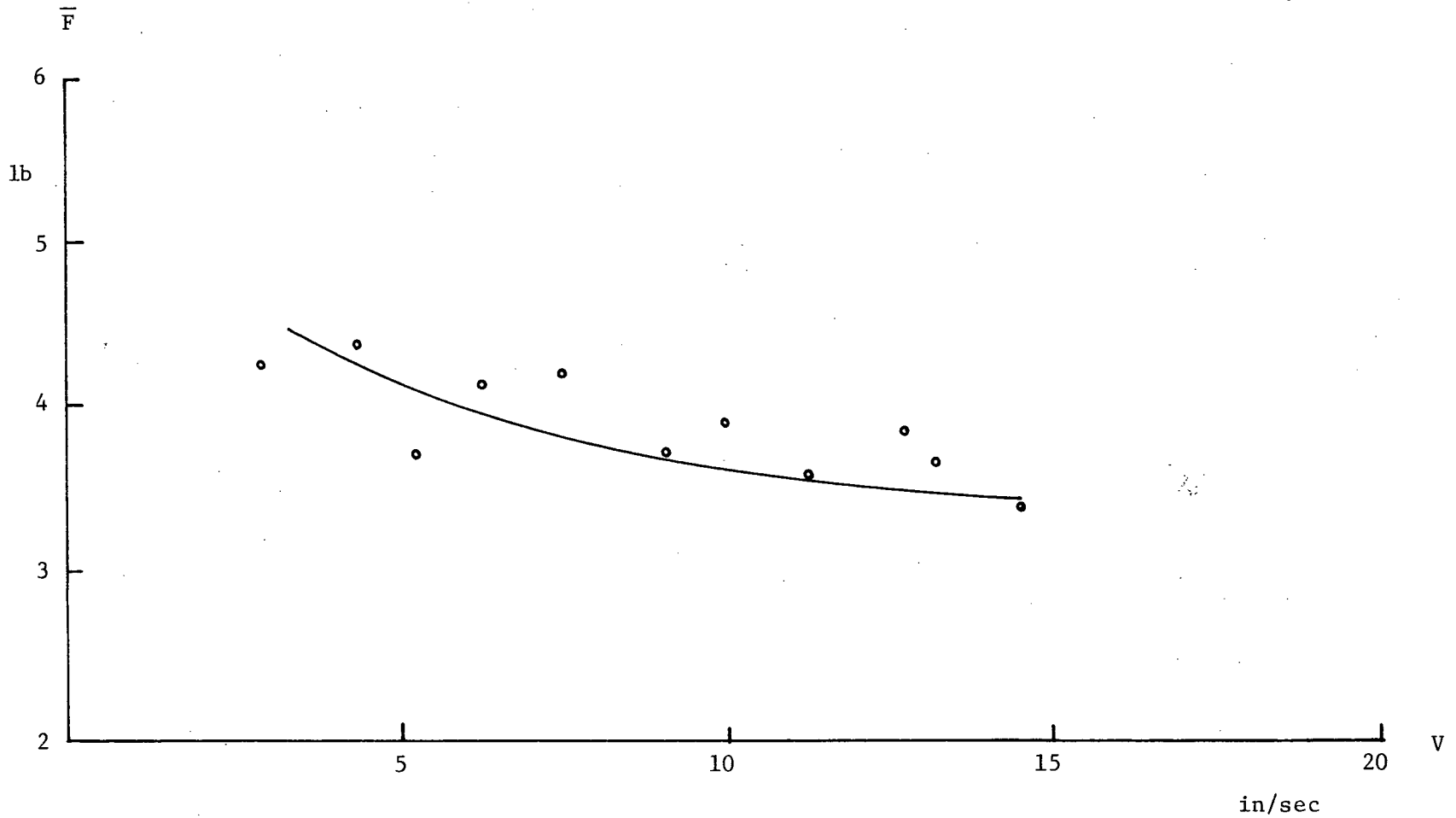

Fig. 4.3.3 (a) Nominal Cutting Force versus Surface Speed for $t_1 \cong 0.005$ in

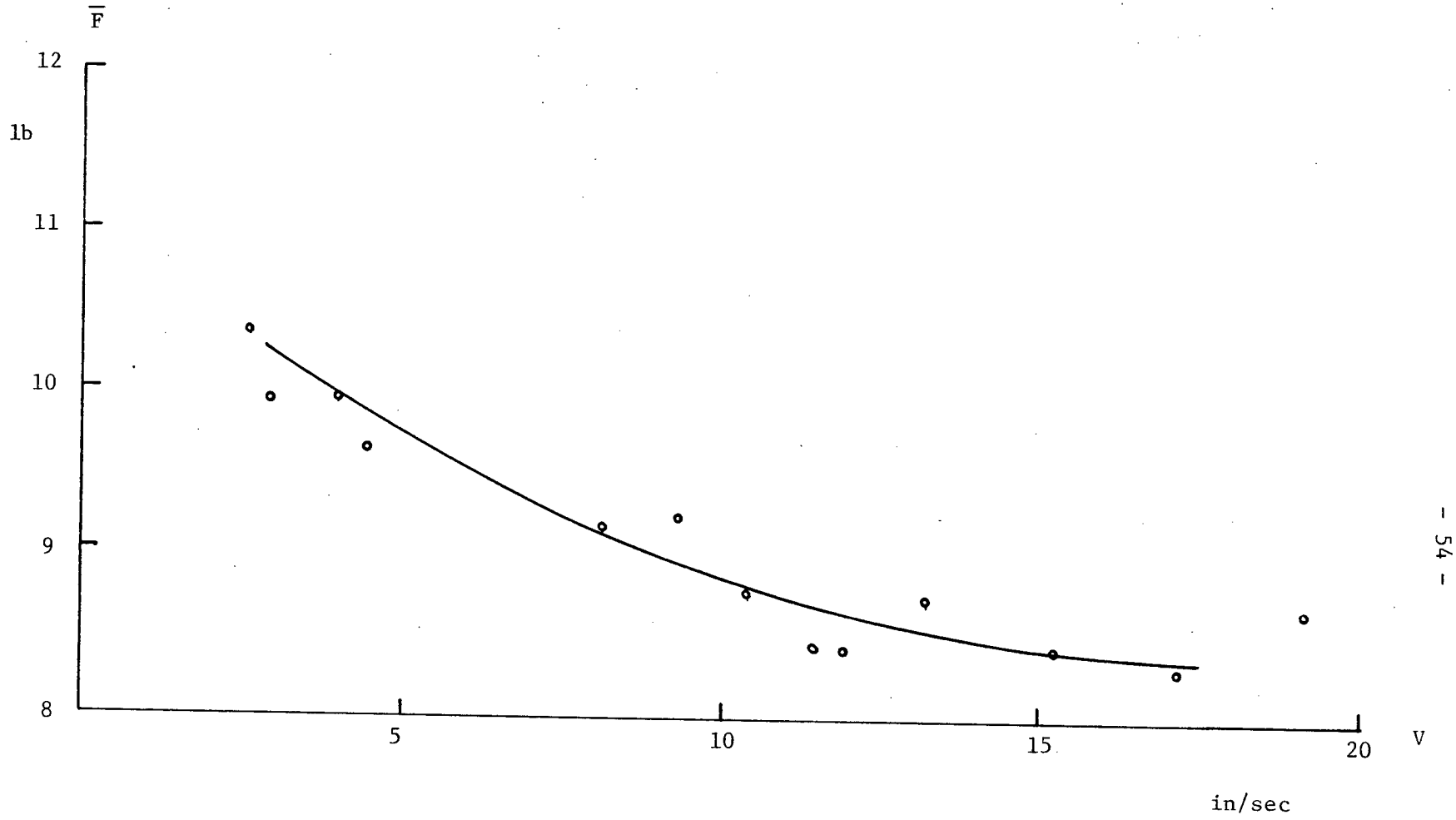

Fig. 4.3.3 (b) Nominal Cutting Force versus Surface Speed fot $t_1 \cong 0.013$ in

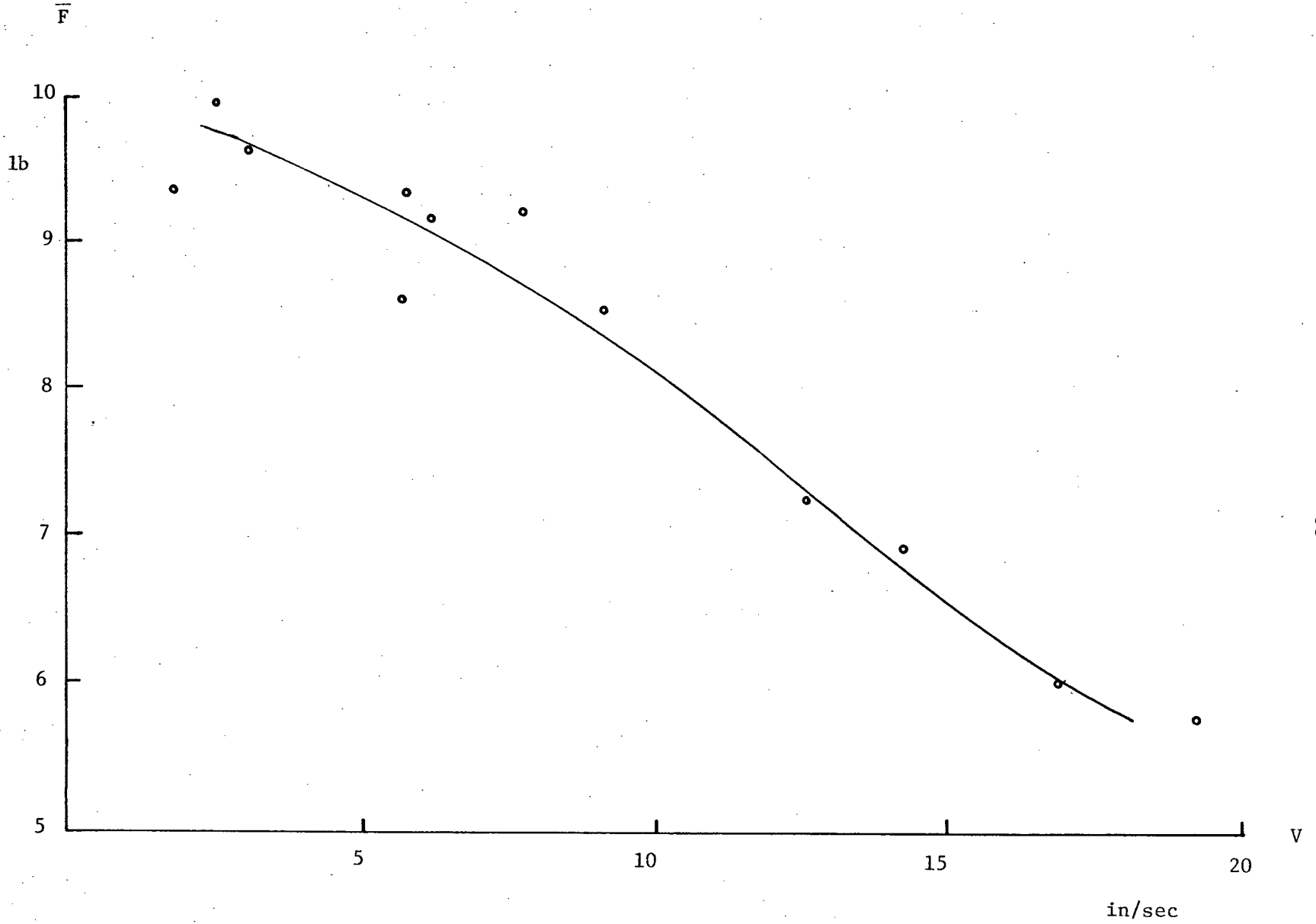

Fig. 4.3.3 (c) Nominal Cutting Force versus Surface Speed for $t_1 \cong 0.022$ in

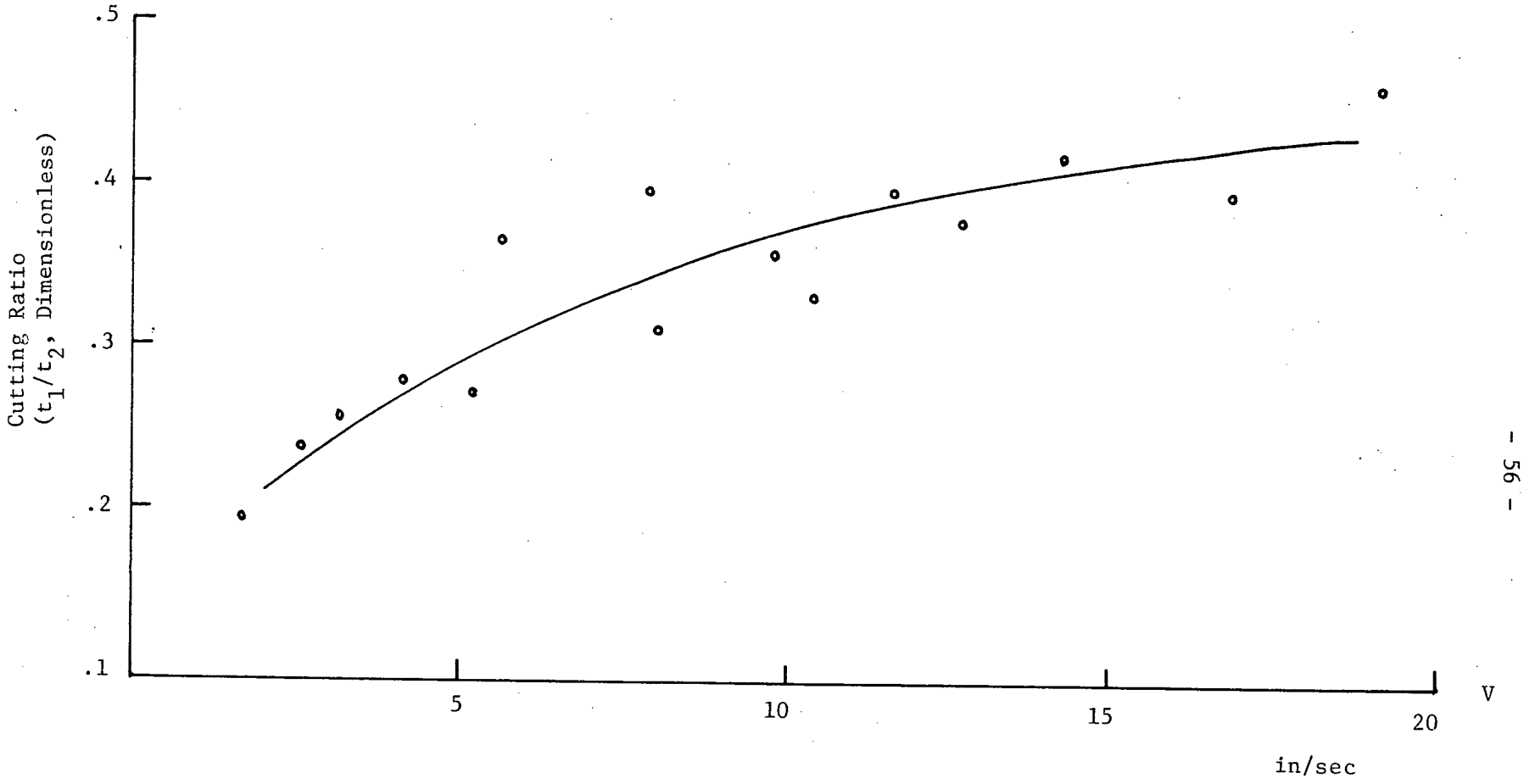

Fig. 4.3.4 Cutting Ratio versus Surface Speed for $t_1 \cong 0.013$ in

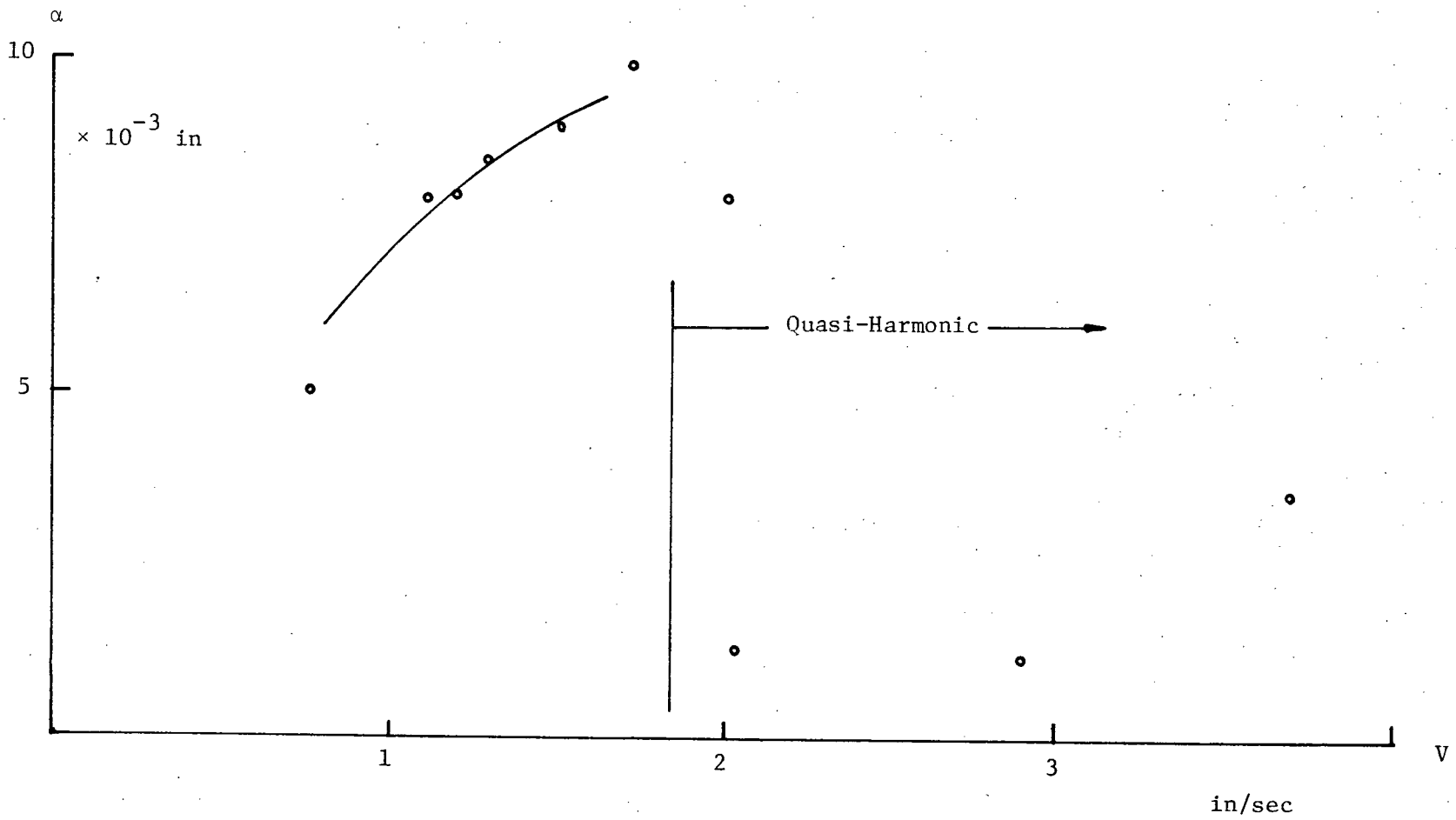

Fig. 4.4.1 Stick Slip Friction-Induced Vibration

(Fig. 4.4.2). At the speeds greater than 15 in/sec , the amplitude was neglible which suggest the metal-cutting equivalent of pure sliding in friction. The metal-cutting quasi-harmonic vibration was observed in the same speed range and behaved in similar manner, which suggested the concept that self-induced chatter is friction actuated.

The apparatus delivered insufficient torque for cutting at very low surface speed (less than 3 in/sec). Therefore, metal-cutting in the range of speed where stick-slip vibration is important was not carried out. Modification of the present apparatus to allow further research in this area is clearly desirable.

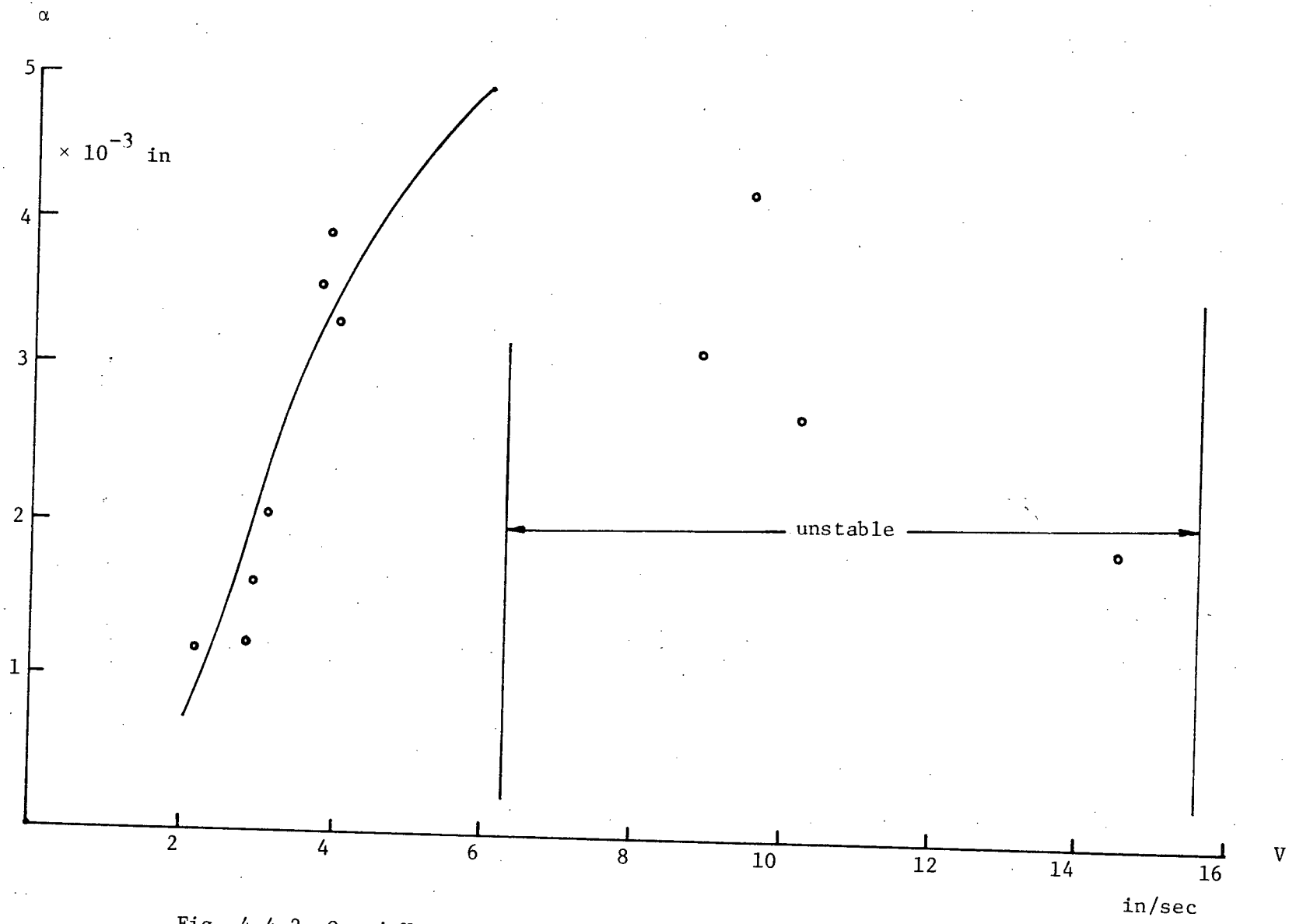

Fig. 4.4.2 Quasi-Harmonic Friction-Induced Vibration

CHAPTER V

5.1 Conclusion

In overall summary of the research, the following conclusions may be listed :

a. Metal cutting chatter was found to occur in the same surface speed range and behaved in similar manner as of the friction-induced quasi-harmonic vibration. Metal cutting in the 'stick-slip' speed range was not investigated due to the inadequacy of the apparatus.

b. A reliable apparatus with good vibration isolation was developed to investigate self-excited chatter in metal cutting. The one-cycle instrumentation techniques [17] were successfully adapted to the present apparatus. It is capable of recording the phase plane and dynamic force-velocity characteristic curve in a single cycle of oscillation.

c. It is possible to apply the method of graphical construction of phase plane developed by Dudley and Swift [19] once the dynamic force-velocity characteristic curve is obtained. The constructed phase plane is in close agreement with experimental results.

d. The dynamic characteristic curve has demonstrated that the overall damping for the cutting system is alternately positive and negative. Positive damping is encountered as the tool bit moves away from the neutral position, thus restraining amplitude growth. Negative damping is encountered as the tool bit moves towards the neutral position, thus providing

energy to maintain the oscillation.

e. The average cutting force, cutting ratio and frequency versus surface speed curves are in agreement with previous workers.

5.2 Suggestions for Future Research

There are two aspects of the present apparatus which can be improved. Firstly, the surface speed can be extended to perform metal cutting in the 'stick-slip' range and a finer speed control should be used to study metal cutting behavior in the low speed range. Secondly, an alternative geometrical design can be used to eliminate the effects of curvature.

A design shown in Fig. 5.2.1 can be used as an apparatus for chatter experiments. The tool bit is held between two rigid beams which are attached around the same axis as the workpiece disc. Elasticity may be provided by torsional springs and external dampers can be added. In this manner, curvature effects are completely eliminated. Various parameters can be studies individually, e.g. effects of varying depth of cut, rake angle, of different stiffness and damping etc.. A smaller workpiece disc can be used, thus reducing cost and the problem of balancing.

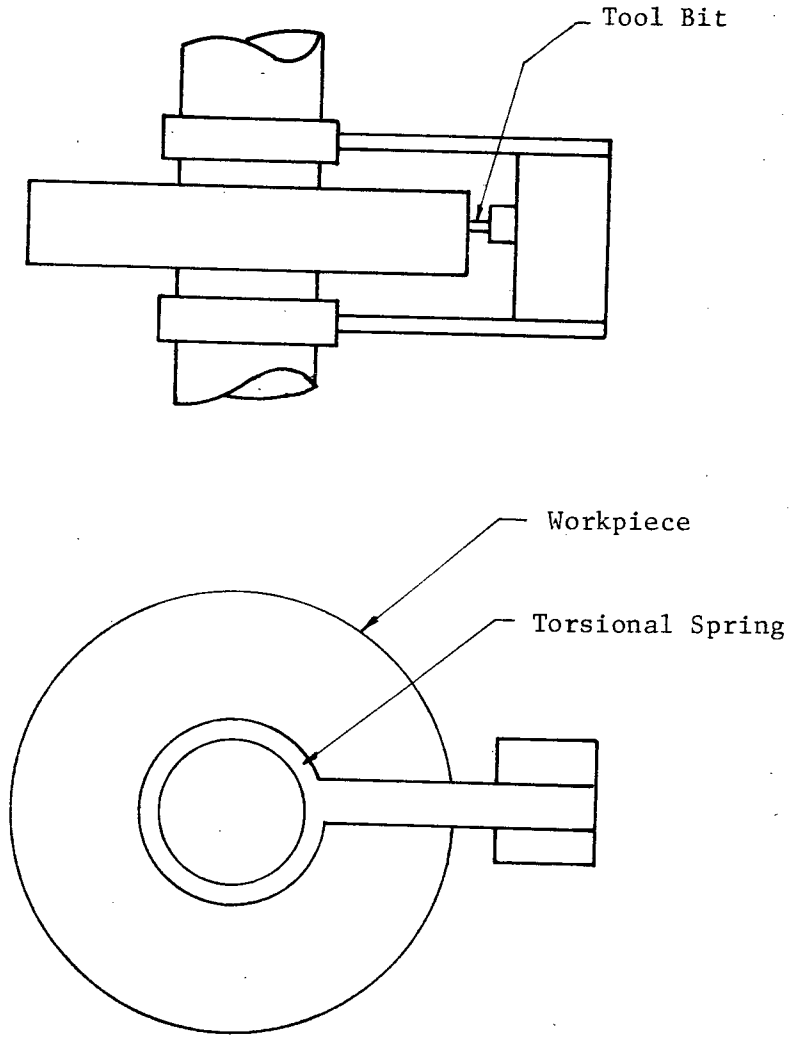

Fig. 5.2.1 Suggested Apparatus for Future Research

REFERENCES

1. Den Hartog, J.P., "Mechanical Vibration", McGraw-Hill Book Company, New York, N.Y., 1947.

2. Hahn, R.S., "Metal-Cutting Chatter and Its Elimination", Trans. ASME, Vol. , 1953, p. 1073.

3. Arnold, R.N., "The Mechanism of Tool Vibration in Cutting Steel", (Cutting Tool Research : Report on Subcommittee on Carbide Tools) Proc. I. Mech. E., Vol. 154, 1946, pp. 261-276.

4. Taylor, E.W., "On the Art of Cutting Metals", Trans. ASME, 1907, p. 30.

5. Dempster, Smith, "Cutting Tools", Trans. Manchester Assoc. Eng., 1911, p. 133.

6. Doi, S., "Chatter of Lathe Tool", J. Soc. Mech. Eng. Japan, Vol. 3, No. 10, 1937, p. 94.

7. American Society of Mechanical Engineers, 1939 Manual of Cutting on Metals.

8. Albrecht, P., "Self-Induced Vibrations in Metal Cutting", Trans. ASME, Jour. Eng. for Industry, Vol. 84, Series B, No. 4, Nov., 1962, p. 405, (Paper No. 55-SA-22).

9. Doi, S. and Kato, S., "Chatter Vibration of Lathe Tools", Trans. ASME, Vol. 78, 1956, p. 1127.

10. Shaw, M.C. and Holken, W., "Über Selbsterregte Schwingungen bei der Spunenden Bearbeitung", Industrie-Anzeiger, Vol. 70, No. 63, Aug., 1957, pp. 35-40.

11. Tobias, S.A., "Machine-Tool Vibration", London, Blackie, 1965, 351p.

12. Chisholm, A.J., "The Cause of Chatter Vibrations", Machinery (London), Vol. 75, 1916, July, 1949, pp. 51-53.

13. Merritt, H.E., "Theory of Self-Excited Machine-Tool Chatter", J. of Eng. for Industry, Nov., 1965, pp. 447-454.

14. Long, G.W., "Structural Dynamic in Machine Tool Chatter", J. of Eng. for Industry, Nov., 1965, pp. 455-463.

15. Kegg, R.L., "Cutting Dynamics in Machine Tool Chatter", J. of Eng. for Industry, Nov., 1965, 464-470.

16. Lemon, I.R. and Ackerman, P.C., "Application of Self-Excited Machine Tool Theory", J. of Eng. for Industry, Nov., 1965, pp. 471-479.

17. Ko, P.L. and Brockley, C.A., "The Measurement of Friction and Friction-Induced Vibration", ASME Paper No. 70-Lubs-15, 1970.

18. Nakayama, K. and Tamura, D., "Size Effect in Metal-Cutting Force", ASME Paper No. 67-Prod-9, 1967.

19. Dudley, B.R. and Swift, H.W., "Frictional Relaxation Oscillations", The Philosophical Magazine, Series 7, Vol. 40, 1949, p. 849.

20. Waldman, N.E. and Gibbens, R.C., "Machinability and Machining of Metals", First Edition, McGraw-Hill Book Company, INC., 1951.

21. Smithells, C.J., "Metals Reference Book", Fourth Edition, London, Butterworths, 1967.

22 McLachlan, N.W., "Theory of Vibrations", Dover Publication Inc., p. p. 12, 1951.

23. Salje, E., "Self-Excited Vibrations of Systems with Two-Degrees of Freedom", Trans. ASME, Vol. 78, 1956, p. 737.

24. Stoker, J.J., 'Nonlinear vibrations in mechanical and electrical systems.' New York. Interscience Publishers, 1950.

25. Minowsky, N., 'Nonlinear Oscillation ', D.Van Nostrand Company, INC., 1962, 713 p.

Appendix I

CALIBRATION OF APPARATUS

(1) System Parameters

Steel Beam $0.2" \times 1"$

$E = 30 \times 10^6$ lb/in^2

$w = 1"$, $h = 0.2"$

$\ell_1 = 1.7"$, $\ell_2 = 1.5"$ (not including the protruding part of the tool bit)

$m = 2.48$ lb

$m_b = 0.113$ lb

$$\delta_a = \frac{P\ell_1^3}{3EI}$$

Assume the tool holder, tool bit, accelerometer, the top part of the velocity transducer and two head weights form a perfectly rigid mass m as shown in Fig. A.I.1. The natural frequency of the system can be estimated from the equation given in [22]

$$\omega_n = \left(\frac{S_b}{m} \right)^{1/2} \left(1 - \frac{33\ m_b}{280\ m} \right)$$

where S_b = Equivalent stiffness at b ;

m_b = Mass of Cantilever Beam.

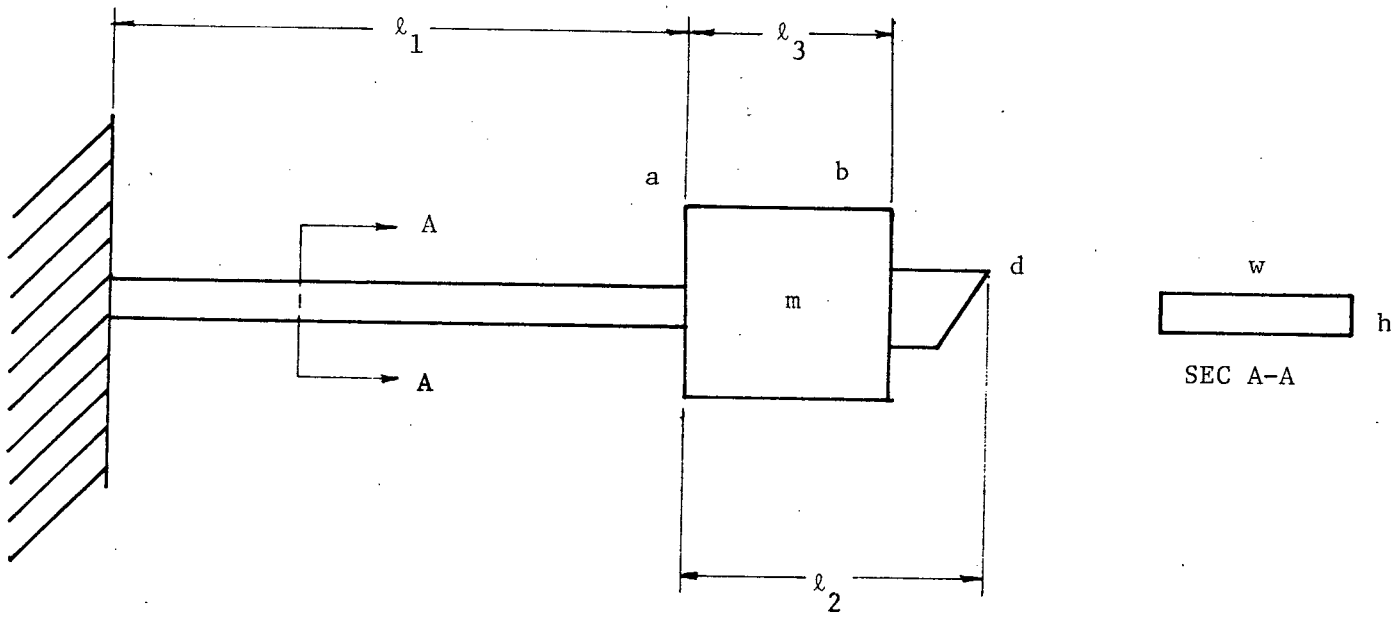

Fig. A.I.1 Schematic Diagram of Tool Holder

The deflection and slope at a due to a force P acting at b are :

$$\delta_a' = \frac{P\ell_1^3}{3EI} + \frac{P\ell_2\ell_1^2}{2EI} = \delta_a\left(1 + \frac{3}{2}\frac{\ell_2}{\ell_1}\right)$$

$$\theta_a' = \frac{P\ell_1^2}{2EI} + \frac{P\ell_2\ell_1}{EI} = \theta_a\left(1 + 2\frac{\ell_2}{\ell_1}\right)$$

Static deflection at b due to P acting at a is :

$$\delta_b = \delta_a' + \theta_a'\ell_2 = \delta_a\left(1 + 3\frac{\ell_2}{\ell_1} + 3\left(\frac{\ell_2}{\ell_1}\right)^2\right)$$

$$S_b = \frac{P}{\delta_b} = 2040 \text{ lb/in}$$

$$\omega_n = 561 \text{ rad/sec}$$

$$= 89.5 \text{ Hz} .$$

The experimentally recorded damped natural frequency of the system is :

$$\omega = 95 \text{ Hz} = 596.6 \text{ rad/sec}$$

Assume the protruding tool bit to be also regid. Then, if a force P is applied at the tool bit, the deflection at d is given by :

$$\frac{\delta_d}{P} = \delta_a\left(1 + 3\frac{\ell_2}{\ell_1} + 3\left(\frac{\ell_3}{\ell_1}\right)^2\right)$$

$$= 9.59 \times 10^{-4} \text{ in.}$$

Therefore $S_d = 1040$ lb/in.

The experimentally measured stiffness is :

$$S_d = 855.6 \text{ lb/in.}$$

(2) Determination of System Damping Coefficient

(a) Logarithmic Decrement Method

In order to determine system damping, the elastic beam was given an initial displacement and then released in free vibration with the tool clear of the workpiece. Oscilloscope records of free vibration were obtained for three similar tests. The logarithm of the vibration amplitudes were plotted versus the number of cycles. The curve was found to be almost linear thus suggesting that the damping coefficient of the system was proportional to the velocity of the vibration. From each test the amplitudes of vibration of every twentieth cycle were recorded and the ratio between consecutive amplitudes was calculated. The average amplitude ratio and the frequency from five tests were used for determining the damping coefficient.

For twenty intervals, we have

$$\frac{x_n}{x_{n+20}} = \frac{e^{-\Delta t}}{e^{-\Delta(t+20\pi/\omega)}} = e^{20\pi\Delta/\omega}$$

or $$\Delta = \frac{\omega}{20\pi} \text{Log}_e\left(\frac{x_n}{x_{n+20}}\right)$$

and $$\omega_n^2 = \omega^2 + \Delta^2 \quad .$$

From experimental results we have

$$\frac{x_n}{x_{n+20}} = 1.410$$

and $\omega = 95$ Hz .

Therefore $\Delta = 1.63$ rad/sec.

The equivalent mass of the system :

$$m = k/\omega_n^2 = 0.923 \text{ lbm}$$

The damping coefficient of the system :

$$r = 2m\Delta = 0.00778 \text{ lb-sec/in} .$$

The coefficient for critical damping :

$$r_c = 2m\omega_n = 2.86 \text{ lb-sec/in} .$$

(b) Force-velocity Gradient during Damped Free Vibration

Since $m\ddot{x} + r\dot{x} + kx = 0$

$$r = \frac{m\ddot{x} + kx}{-\dot{x}} ,$$

which is the force-velocity gradient and could be obtained directly from the phase plane.

Appendix II

CALIBRATION OF INSTRUMENTATION

(1) Displacement

Calibration of displacement was done in a manner as shown in Fig. A.II.1. The weight pan was hung on a string which was fastened to a screw on a 3/8" shank. The screw was at the same distance from the tool holder as the tool bit. Deflection was caused by adding dead weights to the pan. To measure the deflection, a depth micrometer was rigidly mounted with the spindle vertical. A calibration curve was obtained by plotting beam deflection versus dead weight. A steel bar, which would cause a deflection of .002 in was used to check the instrumentation before tests.

(2) Velocity

For a damped free vibration system the amplitude of vibration is

$$x = Ae^{-\Delta t}\cos(qt + \phi)$$

$$\dot{x} = Ae^{-\Delta t}[-\Delta\cos(qt + \phi) - q\sin(qt + \phi)]$$

$$\ddot{x} = Ae^{-\Delta t}[-(\Delta^2 - q^2)\cos(qt + \phi) + 2\Delta q\sin(qt + \phi)]$$

where $\Delta = r/2m$ and $q = \sqrt{w^2 - \Delta^2}$.

From Appendix I, $q >> \Delta$.

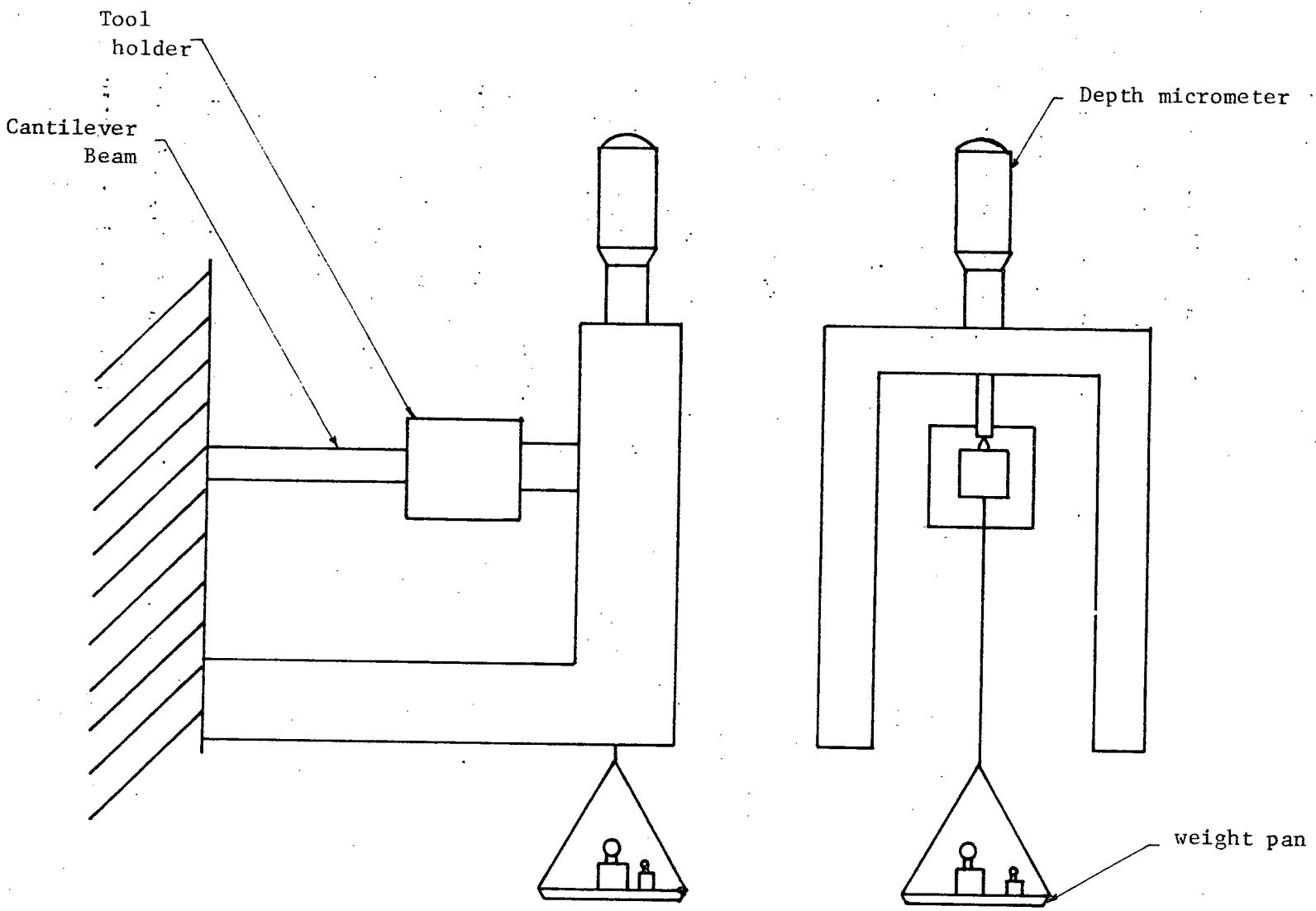

Fig. A.II.1 Method of Calibration of Displacement

Therefore, for calibration purposes, it is sufficient to consider $\dot{X} = qX$ and $\ddot{X} = q^2X$, where X, $\dot{X}$ and $\ddot{X}$ are the peak values of x, $\dot{x}$ and $\ddot{x}$. The calibration of the velocity signal was fulfilled by performing a free oscillation test of the vibration system. A x-$\dot{x}$ phase plane plot was obtained from the oscilloscope. The D.C. output signals of x and $\dot{x}$ were recorded. The actual displacement in inches was obtained from the calibration described in Appendix II (1). Knowing q from Appendix I, the actual velocity in terms of in/sec was obtained from $\dot{x} = qx$. Comparing the velocity in in/sec with its corresponding D.C. signal, a relationship in terms of D.C. output and in/sec could be obtained.

(3) Accelaration

The accelerometer is a commercial unit and has a pre-calibrated output of 0.1 volt per g. However, the position of the accelerometer is 1.44 in behind the tip of the tool bit, where displacement calibration was carried out. In addition, scaling of the acceleration force term and the spring force term was required so that $\dot{x} = 0$, $m\ddot{x} + kx = 0$. The scaling procedure was carried out by applying the displacement and accelerometer signals to the differential amplifier of the oscilloscope and the velocity signal to the horizontal display amplifier during free vibration test and adjusting the gain control of the bridge amplifier meter until the combined and accelerometer signal formed a straight line. From Appendix II (2), we have $\dot{x} = xq^2$. Knowing x and q, a relationship in terms of D.C. output per in/sec^2 could be obtained.

Appendix III

SPECIMEN COMPOSITION AND MECHANICAL PROPERTIES

Mechanical properties of 70/30 brass at room temperature are given by [21] :

Nominal Composition (%) Cu 70.10, Zn 29.83

Specification :	B.S.	U.S.
	267	A.S.T.M.
	S.T.A. 18	B 36 - 40 T
		B 19 - 40 T
		S.A.E. 70
		Grad. A

Condition ..... Strip

Annealed

Holf-Hardened C.R. : 15% reduction

Hardened C.R. : 30% reduction

Limit of proportionality (psi)	6,720
0.1% Proof Stress (psi)	12,300
U.T.S. (psi)	46,300
Elongation (2 in gauge length (%))	67.5
Shear Stress (psi)	33,400
Brinell Hardness	62
Vicker's Hardness	66
Modulus of Elasticity (psi)	15×10^6